International Journal of Applied Pharmaceutics

ISSN- 0975-7058 Vol 16, Issue 5, 2024

Original Article

INVESTIGATING MULTITARGET POTENTIAL OF *MUCUNA PRURIENS* AGAINST PARKINSON'S DISEASE: INSIGHTS FROM MOLECULAR DOCKING, MMGBSA, PHARMACOPHORE MODELLING, MD SIMULATIONS AND ADMET ANALYSIS

ZAKIYA FATHIMA C.[1], JAINEY P. JAMES[1*], MAHENDRA GOWDRU SRINIVASA[1], SINDHU T. J[1], MARIYAM JOUHARA B. M.[1], B. C. REVANASIDDAPPA[1], SUDEEP D. GHATE[2]

[1]Department of Pharmaceutical Chemistry, NGSM Institute of Pharmaceutical Sciences (NGSMIPS), Nitte (Deemed to be University), Deralakatte, Mangaluru-575018, Karnataka, India. [2]Department of Microbiology, Central Research Laboratory, KS Hegde Medical Academy (KSHEMA), NITTE Deemed to be University, Mangalore-575018, (Karnataka) India

[*]Corresponding author: Jainey P. James; [*]Email: jaineyjames@gmail.com

Received: 16 May 2024, Revised and Accepted: 02 Jul 2024

ABSTRACT

Objective: *Mucuna pruriens* (Velvet beans) is a leguminous plant recognised in Vedic therapy as an anti-Parkinsonism agent. The plant is known as the natural reservoir for levodopa. The study aims to evaluate the multitarget inhibitory potency of active constituents present in *Mucuna pruriens* using *in silico* tools.

Methods: The phytoconstituents present in *Mucuna pruriens* were retrieved from the IMPPAT database. The physicochemical and toxicity parameters of phytoconstituents were evaluated using Qikprop and ProTox-3. The inhibitory potential of phytoconstituents on the enzymes Monoamine Oxidase-B (MAO-B), Acetylcholinesterase (AChE), and Catechol-O-Methyltransferase (COMT) was evaluated using *in silico* techniques, including molecular docking, pharmacophore modelling, and molecular dynamics simulations, conducted with Schrödinger software programs.

Results: The active constituents comply with Lipinski's rule for drug-likeness. Further, the molecular docking studies revealed the phytoconstituent luteolin and acacetin showed promising multitargeted inhibitory properties. Especially luteolin (-11.504 kcal/mol) and acacetin (-10.620 kcal/mol) have obtained excellent docking scores with MAO-B, whereas the known drug levodopa showed a docking score of-8.501 kcal/mol. The pharmacophore modelling revealed that donor, acceptor, and aromatic features present in luteolin and acacetin are the essential pharmacophoric features accountable for biological activity. The simulation study generated the stability of the protein-ligand complex and found that luteolin showed a stable complex with MAO-B.

Conclusion: Based on these findings, the result of the current study can be used to develop a novel luteolin-based drug for treating Parkinson's disease with preferred structural modification. However, additional and more comprehensive research is required on this compound.

Keywords: *Mucuna pruriens,* Multitarget, Molecular docking, Pharmacophore modelling, Molecular dynamic simulation, Luteolin, Acacetin, Parkinsons' disease

DOI: https://dx.doi.org/10.22159/ijap.2024v16i5.51474 Journal homepage: https://innovareacademics.in/journals/index.php/ijap

INTRODUCTION

Most of the world's population uses plant-based medicine to treat various ailments as an essential component of culture and tradition. This therapeutic approach is highly demanded due to several factors, including the accessibility, affordability, and availability of traditional medicinal plants [1]. The *Mucuna pruriens* (Velvet beans) is a leguminous plant, of Fabaceae family. The plant, generally found in tropical and subtropical regions, is a well-known therapeutic agent for Parkinson's Disease (PD) [2, 3] in Ayurvedic medicine. The plant's leaves, roots, and seeds are used in traditional remedies. *Mucuna pruriens* were reported to have antioxidant [4], antivenom [5], neuroprotective activities [6], antidiabetic [7], anticholesterolemic [8], anti-inflammatory [9], antimicrobial [10], anticancer activity [11] and to treat erectile dysfunction [12].

The *Mucuna pruriens* is a natural source of levodopa, which is considered the golden strand for treating PD [13]. Several studies have been reported describing the potential role *of Mucuna pruriens* in treating PD. It is characterised by abnormal aggregates of a protein called Lewy bodies and exhibits several common traits, including oxidative stress, misfolded proteins, protein aggregation, excitotoxicity, neuroinflammation, and neuronal loss [14]. The neuropathological features of PD are associated with dysfunction in the cholinergic and dopaminergic systems. Consequently, current therapeutic strategies for PD primarily target the improvement of these dysfunctions.

The leading underlying cause of PD is the gradual depletion of dopamine resulting from extensive degeneration of dopaminergic neurons [15]. Treatment strategies primarily focus on enhancing dopaminergic levels and identifying non-dopaminergic medications to delay the physical and psychological symptoms associated with the condition. These therapeutic interventions encompass drugs targeting the dopaminergic system, such as levodopa, dopamine agonists, Monoamine Oxidase-B (MAO-B) inhibitors, and Catechol-O-Methyltransferase (COMT) inhibitors, as well as non-dopaminergic medications like anticholinergics and glutamate antagonists [16]. Hence, the Multi-Target Directed Ligands (MTDLs) approach gains importance in neurochemistry, which aims to create compounds that can act on multiple targets in neurodegenerative diseases like PD [17]. Traditional drug design, which focuses on one target per drug, isn't effective for complex diseases like neurodegeneration [18]. The reliance on a single drug targeting a single protein increases susceptibility to resistance development due to mutations in active target sites. Now, researchers focus on small molecule-based MTDLs, which can influence multiple pharmacologically significant targets within the Central Nervous System (CNS) while exhibiting low affinity towards other cellular proteins [19]. These MTDLs are characterised by favourable physicochemical and toxicological properties, reducing the likelihood of adverse effects. Additionally, MTDLs have the potential for synergistic or additive effects, demonstrating a unified pharmacokinetic and pharmacodynamic profile [20].

The current study aims to analyse the multitargeting inhibitory potential of phytoconstituents present in *Mucuna pruriens* against the targets MAO-B, AChE, and COMT by employing *in silico* tools. Additionally, the study explores the pharmacological implications of *Mucuna pruriens*, shedding light on its potential for treating PD and

related conditions. The investigation encompasses assessing pharmacokinetic properties, docking, pharmacophore modelling, binding free energy calculation, and Molecular Dynamics (MD) simulation study. The resulting data provide insights into the crucial phytoconstituents responsible for inhibitory properties of overexpression of the enzymes involved in PD.

MATERIALS AND METHODS

In silico platform

All the works were performed using Maestro 13.5.128 version of Schrödinger 2023-1, LLC, New York. The workstation machine runs with Linux –x86_64 as the operating system, of Intel core i7 (octa-core) processor, with 16 GB RAM, 1 TB Hard disk, and a 64-bit System. The molecular dynamics were performed using DESMOND (Schrodinger Inc., USA). Online tools like PASS Predictor, ProTox-3, and Swiss target predictor were utilised.

Preparation of ligand library

The phytoconstituents of *Mucuna pruriens* were selected from the IMPPAT database (Indian Medicinal Plants Phytochemistry and Therapeutics). The SMILES and PubChem ID of the phytoconstituents were extracted from the PubChem database. The data is tabulated in table 1.

Prediction of ADME and physicochemical properties

QikProp module of Schrödinger suite 2023-1 was utilised to determine the ADME and physicochemical properties, which screens the ligands for their drug-likeness and bioavailability [21].

Toxicity prediction

The toxicity profile of the constituent was assessed using the ProTox-3 (https://comptox.charite.de/protox3/index.php?site=compound_input) free online tool [22]. The SMILE strings representing the bioactives were inputted into the web page, and the predict button was clicked to generate the results.

Molecular docking

Ligand preparation: The SMILES were imported to the Maestro interface of Schrödinger. LigPrep utilises the OPLS-3 force field to generate low-energy conformations of ligands and the 3D structures of ligands were built at an ionisation state of pH 7 [23].

Protein preparation: The 3D crystal structure of protein structure of human MAO-B in complex with the selective inhibitor safinamide (2V5Z) [24], human AChE in complex with huprine W and fasciculin 2 (4BDT) [25], and crystal structure of human COMT complexed with S-Adenosyl Methionine (SAM) and 3,5-dinitro catechol (3A7E) [26] was downloaded and viewed with the maestro interface of Schrödinger software. The structure of the target protein was rectified using the Protein Preparation Wizard of Maestro. The complexes containing covalent interaction between protein and ligand were initially eliminated. It is necessary to prepare protein thoroughly before molecular docking; hence, the missing hydrogen atoms were incorporated to achieve proper bond order. Active site water molecules beyond 5 Å were removed. The away side chain atoms were added, and gaps in the protein structure were rectified. The energy-minimised protein was prepared using the OPLS_2005 force field [27].

Receptor grid generation: The grid box was constructed around the active site of the minimised protein using the Glide panel. This grid precisely delineates the three-dimensional space for potential ligand binding [27].

Docking: Docking of receptor-ligand assists in identifying the optimal binding configurations of ligands within the target. The phytoconstituents were docked against the targets (2V5Z, 4BDT, 3A7E) utilising an extra precision (XP) algorithm incorporating flexible ligand docking. Determining the most favourable confirmation relies on achieving the lowest binding energy or markedly negative binding affinity magnitude [28].

Prime MM-GBSA binding free energy

The prime module was utilised to determine the binding free energy for protein-ligand complexes. This module computes the overall free energy in terms of dGbind (kcal/mol), considering molecular mechanics energies and solvation models for nonpolar and polar solvation [29].

Pharmacophore modelling

The two compounds with the most elevated docking scores were selected for pharmacophore modelling study, utilising phase application [30]. This receptor-based technique evaluates the essential pharmacophoric features of ligands responsible for the bioactivity.

MD simulation

The MD study used the desmond module from Schrödinger Inc., USA. The Berendsen thermostat and barostat methods were employed for a 150 ns simulation. The simulation system utilised the NPT ensemble with a temperature of 300 K and pressure of 1.01325 bars. Before the simulation, the protein-ligand complex underwent energy minimization. Partial charges for the complex were determined during this process. The solvated system was placed in a TIP3P orthorhombic box. Neutralisation of each system was achieved by adding 0.15 M NaCl to the buffer. The system was further prepared using Protein Preparation, Ligand preparation, and Epik tools in desmond. Initial simulations were performed for ten ns in an NPT ensemble with a temperature of 300 K and pressure of 1.01325 bars. Molecular dynamics simulations were subsequently extended to 150 ns, with trajectory information collected for the remaining 2.0 ns [31]. Trajectory information generated plots depicting RMSD, RMSF, and hydrogen bonds. These plots provided insights into the stability and dynamics of the protein-ligand complex throughout the simulation. The comprehensive approach, including energy minimisation, explicit solvation, and advanced simulation parameters and tools, adds rigour to the study. The 150 ns simulation duration allows for a detailed analysis of the dynamics and stability of the best-docked protein-ligand complex. Including trajectory information further enhances the understanding of the system's behaviour.

PASS analysis

The virtual screening of the highest docked compound was carried out using the online software Prediction of Activity Spectra for Substances (PASS) (http://www.way2drug.com/). The program predicts the bioactivity based on the Structural Activity Relationship (SAR) from the training sets [32]. The result is generally represented as Pi and Pa, which gives the probability for the activity and inactivity of the compound, respectively.

RESULTS

Physicochemical properties

The pharmacokinetic properties and the drug-like characteristics of the phytoconstituents are illustrated in table 2.

The drug-like characteristics of the phytoconstituents evaluated based on Lipinski's Rule of Five (RO5), the molecular weight (≤500 daltons), the partition coefficient (≤5), and the count of hydrogen bond donors and acceptors should be ≤5 and ≤10, respectively. On analysis, a few showed violations of one parameter but not more than one. Hence, all the compounds can be considered drug-like candidates.

The PSA (Polar Surface Area) is a descriptor that measures the portion of polar atoms occupied in the molecule's surface area occupied by polar atoms, mainly oxygen and nitrogen, as well as any attached hydrogen atoms [33]. This parameter is crucial in predicting bioavailability, as compounds with higher PSA values often struggle to penetrate cell membranes, potentially resulting in lower bioavailability. All phytoconstituents exhibited PSA values falling within the range of 7-200Å^2.

Table 1: Smiles and structures of phytoconstituents present in *Mucuna pruriens*

S. No.	Phytoconstituents	PubChem ID	Smiles	Structures
1.	Luteolin	5280445	C1=CC(=C(C=C1C2=CC(=O)C3=C(C=C(C=C3O2)O)O)O)O	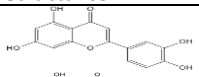
2.	Acacetin	5280442	COC1=CC=C(C=C1)C2=CC(=O)C3=C(C=C(C=C3O2)O)O	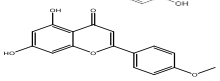
3.	Arachidic acid	10467	CCCCCCCCCCCCCCCCCCCC(=O)O	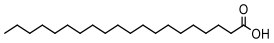
4.	Genistein	5280961	C1=CC(=CC=C1C2=COC3=CC(=CC(=C3C2=O)O)O)O	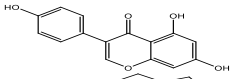
5.	Sterol	1107	C1CC2CCC3C4CCC(CC4CCC3C2C1)O	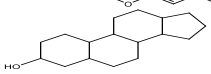
6.	Oleic acid	445639	CCCCCCCCC=CCCCCCCCC(=O)O	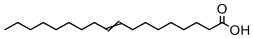
7.	N, N-dimethyltryptamine	6089	CN(C)CCC1=CNC2=CC=CC=C21	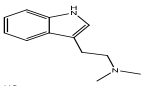
8.	Dopamine	681	C1=CC(=C(C=C1CCN)O)O	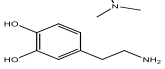
9.	Stearic acid	5281	CCCCCCCCCCCCCCCCCC(=O)O	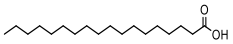
10.	Linoleic acid	5280450	CCCCCC=CCC=CCCCCCCCC(=O)O	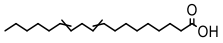
11.	Glutathione	124886	C(CC(=O)NC(CS)C(=O)NCC(=O)O)C(C(=O)O)N	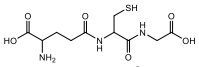
12.	Levodopa	6047	C1=CC(=C(C=C1CC(C(=O)O)N)O)O	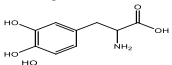
13.	Ascorbic acid	54670067	C(C(C1C(=C(C(=O)O1)O)O)O)O	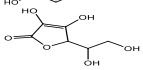
14.	Palmitic acid	10889	CCCCCCCCCCCCCCCCOC(=O)CCCCCCCCCCCCCCC	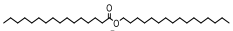
15.	Gallic acid	811292	C1=C(C=C(C(=C1O)O)O)C(=O)O	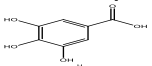
16.	Bufotenine	10257	CN(C)CCC1=CNC2=C1C=C(C=C2)O	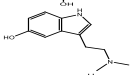
17.	Serotonin	5202	C1=CC2=C(C=C1O)C(=CN2)CCN	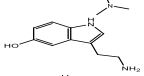
18.	Tryptamine	1150	C1=CC=C2C(=C1)C(=CN2)CCN	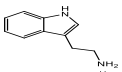
19.	N, N-dimethyl-5-methoxy tryptamine	1832	CN(C)CCC1=CNC2=C1C=C(C=C2)OC	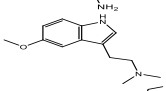
20.	Beta-sitosterol	222284	CCC(CCC(C)C1CCC2C1(CCC3C2CC=C4C3(CCC(C4)O)C)C)C(C)C	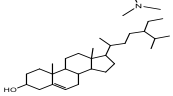
21.	Myristic acid	11005	CCCCCCCCCCCCCC(=O)O	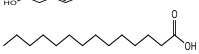
22.	Coumarin	323	C1=CC=C2C(=C1)C=CC(=O)O2	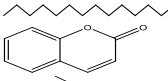
23.	Nicotine	89594	CN1CCCC1C2=CN=CC=C2	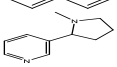
24.	Stigmasterol	5280497	CCC(C=CC(C)C1CCC2C1(CCC3C2CC=C4C3(CCC(C4)O)C)C)C(C)C	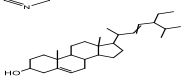
25.	Vernolic acid	6449780	CCCCCC1C(O1)CC=CCCCCCCCC(=O)O	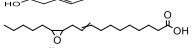
26.	9H-Pyrido[3,4-B]indole	64961	C1=CC=C2C(=C1)C3=C(N2)C=NC=C3	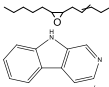
27.	6-methoxy-1-methyl-9H-pyrido[3,4-b]indole	5376026	CC1=NC=CC2=C1NC3=C2C=C(C=C3)OC	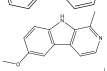
28.	Alpha-amyrenyl acetate	92842	CC1CCC2(CCC3(C(=CCC4C3(CCC5C4(CCC(C5(C)C)OC(=O)C)C)C)C2C1C)C)C	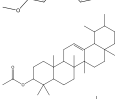
29.	Ursolic acid	64945	CC1CCC2(CCC3(C(=CCC4C3(CCC5C4(CCC(C5(C)C)O)C)C)C2C1C)C)C(=O)O	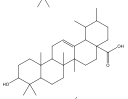
30.	Betulinic acid	64971	CC(=C)C1CCC2(C1C3CCC4C5(CCC(C(C5CCC4(C3(CC2)C)C)(C)C)O)C)C(=O)O	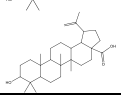

Table 2: Physicochemical properties of phytoconstituent present in *Mucuna pruriens*

Phytoconstituents	Mol. Wt	Donor HB	Acceptor HB	QPlogO/W	PSA	RO5	RO3
Acceptable range	≤500	≤5	≤10	(-2.0 to 6.5)	7– 200	<4	<3
Luteolin	286.24	3.00	4.50	0.95	121.40	0	0
Acacetin	284.26	1.00	3.75	2.49	85.92	0	0
Arachidic acid	312.53	1.00	2.00	6.59	47.03	1	1
Genistein	270.24	2.00	3.75	1.66	96.94	0	0
Sterol	248.40	1.00	1.70	3.83	22.27	0	0
Oleic acid	282.46	1.00	2.00	5.94	49.61	1	1
N, N-dimethyltryptamine	188.27	1.00	2.00	2.46	19.78	0	0
Dopamine	153.18	4.00	2.50	-0.97	70.75	0	0
Stearic acid	284.48	1.00	2.00	5.99	49.91	1	1
Linoleic acid	280.45	1.00	2.00	5.84	49.81	1	1
Glutathione	307.32	4.50	8.00	-3.10	194.03	1	2
Levodopa	197.19	5.00	4.50	-2.48	114.28	0	1
Ascorbic acid	176.12	4.00	7.90	-1.85	125.38	0	0
Palmitic acid	256.42	1.00	2.00	5.21	51.15	1	0
Gallic acid	170.12	4.00	4.25	-0.55	116.15	0	1
Bufotenine	204.27	2.00	2.75	1.68	42.64	0	0
Serotonin	176.21	4.00	1.75	0.21	63.16	0	0
Tryptamine	160.21	3.00	1.00	1.22	40.18	0	0
N, N-Dimethyl-5-methoxy tryptamine	218.29	1.00	2.75	2.47	27.91	0	0
Beta-sitosterol	414.71	1.00	1.70	7.38	22.21	1	1
Myristic acid	146.14	0.00	2.50	1.39	40.57	0	0
Coumarin	228.37	1.00	2.00	4.44	51.54	0	0
Nicotine	162.23	0.00	3.50	1.18	18.09	0	0
Stigmasterol	412.69	1.00	1.70	7.27	22.31	1	1
Vernolic acid	296.44	1.00	4.00	4.86	64.71	0	0
9H-Pyrido[3,4-B]indole	168.19	1.00	1.50	2.34	27.00	0	0
6-methoxy-1-methyl-9H-pyrido[3,4-b]indole	212.25	1.00	1.75	3.08	33.66	0	0
Alpha-amyrenyl acetate	468.76	0.00	2.00	3.62	32.64	1	1
Ursolic acid	456.70	2.00	3.70	8.20	58.00	1	1
Betulinic acid	456.70	2.00	3.70	8.06	58.14	1	1

Mol. Wt-Molecular Weight, Donar HB-Hydrogen Bond Donor, Accept HB-Hydrogen Bond Acceptor, QPlog o/w-Predicted octanol/water partition coefficient, PSA-Polar Surface Area, RO5-Rule of Five, RO3-Rule of Three.

Table 3: Solvent-accessible surface area prediction

Phytoconstituents	SASA	FOSA	FISA	PISA
Luteolin	501.47	0.00	249.28	252.19
Acacetin	516.54	92.16	148.47	275.90
Arachidic acid	755.02	664.31	90.71	0.00
Genistein	476.51	0.00	184.06	292.44
Sterol	502.23	453.31	48.92	0.00
Oleic acid	724.09	606.99	101.69	15.41
N, N-dimethyltryptamine	445.94	196.28	35.48	214.17
Dopamine	365.97	82.36	164.53	119.07
Stearic acid	717.71	620.84	96.87	0.00
Linoleic acid	714.99	583.91	101.97	29.10
Glutathione	554.14	164.70	323.52	0.00
Levodopa	393.83	57.28	233.89	102.65
Ascorbic acid	337.12	81.57	246.04	9.50
Palmitic acid	666.91	558.68	108.23	0.00
Gallic acid	346.56	0.00	255.19	91.36
Bufotenine	456.48	195.43	90.68	170.35
Serotonin	392.03	79.95	143.21	168.86
Tryptamine	383.96	87.50	84.01	212.43
N,N-dimethyl-5-methoxy tryptamine	470.16	297.24	34.38	138.53
Beta-sitosterol	748.16	668.53	48.46	31.16
Myristic acid	600.54	491.32	109.22	0.00
Coumarin	332.39	0.00	72.44	259.95
Nicotine	396.74	218.56	30.76	147.41
Stigmasterol	735.71	657.11	48.73	29.86
Vernolic acid	689.00	565.46	107.71	15.82
9H-Pyrido[3,4-B]indole	375.17	0.00	53.72	321.45
6-methoxy-1-methyl-9H-pyrido[3,4-b]indole	444.09	179.82	38.12	226.14
Alpha-amyrenyl acetate	730.23	671.88	41.50	16.85
Ursolic acid	679.35	574.57	88.50	16.27
Betulinic acid	686.44	571.09	90.66	24.68

SASA-Total solvent accessible surface area, FOSA-Hydrophobic component of the SASA, FISA-Hydrophilic component of the SASA, PISA-π (carbon and attached hydrogen) component of the SASA.

Jorgensen's Rule of Three (RO3) predicts the oral bioavailability of a compound. According to RO3, the QPlogS value should be greater than -5.7, the QPCaco value should exceed 22 nm/s, and the number of primary metabolites should be fewer than 7 [34]. The lesser the violation, the more compounds are likely to be orally available. The other descriptors used to evaluate the oral bioavailability of the compounds are % Human Oral Absorption (%HOA), and Madin-Darby Canine Kidney (MDCK) cell models. Glutathione showed two violations for RO3. Hence, all the selected phytoconstituents were considered to be orally active.

Solvent accessible surface area

Total Solvent Accessible Surface Area (SASA) in square angstroms using a probe with a 1.4 Å radius ranges from 300.0 – 1000.0 Å^2 [35]. All the phytoconstituents showed SASA within the standard range. SASA gives a general measure of the surface accessibility of a molecule to solvent molecules; FOSA, FISA, and PISA provide more specific information. FOSA value (0.0–750.0 Å^2) gives the hydrophobic component, while the FISA value (7.0–330.0Å^2) contributes to the hydrophilic part. The top-scoring compounds, luteolin and acacetin, had greater hydrophilic components in solvent-accessible surface areas and fewer hydrophobic components. PISA represents the π (carbon and attached hydrogen) part (0.0–450.0 Å^2). All the phytoconstituents show values within a reasonable range. The SASA prediction of the phytoconstituent is given in table 3.

Prediction of pharmacokinetic properties

The pharmacokinetic properties, including Absorption, Distribution, Metabolism and Extraction (ADME) parameters of the phytoconstituents, are evaluated using Qiprop [36] and are illustrated in table 4.

Table 4: ADME properties of phytoconstituents

Phytoconstituents	%HOA	QPlogS	QPlogCaco	QPlog MDCK	QPlogKhsa	QPlogBB	CNS	#metab	QPlog HERG
Acceptable range	>80% High <25% Low	-6.5 to-0.5	>500 Great <25 Poor	>500 Great <25 Poor	–1.5 to 1.5	–3.0 to 1.2	–2 to+2	(1-8)	Below –5
Luteolin	61.75	-3.06	42.85	16.43	-0.19	-1.92	-2	4	-5.00
Acacetin	87.88	-3.87	387.14	177.37	0.15	-0.96	-1	3	-5.16
Arachidic acid	100.00	-6.41	346.17	199.90	0.90	-1.54	-2	1	-3.47
Genistein	76.95	-2.94	177.98	76.57	-0.11	-1.27	-2	3	-4.93
Sterol	100.00	-4.61	3403.57	1859.13	0.68	0.09	1	1	-3.21
Oleic acid	92.36	-6.32	272.36	154.25	0.76	-1.50	-2	3	-3.63
N, N-dimethyltryptamine	96.09	-1.95	1138.39	629.61	0.08	0.47	2	2	-5.21
Dopamine	54.02	0.43	67.99	29.94	-0.75	-0.67	-1	5	-4.31
Stearic acid	93.46	-6.04	302.60	172.85	0.73	-1.48	-2	1	-3.41
Linoleic acid	91.72	-6.31	270.71	153.25	0.75	-1.44	-2	4	-3.66
Glutathione	0.00	-0.40	0.06	0.13	-1.74	-2.63	-2	7	1.42
Levodopa	22.77	-0.68	3.78	1.68	-0.96	-1.28	-2	6	-2.38
Ascorbic acid	45.86	-0.63	45.99	17.73	-0.92	-1.66	-2	5	-2.58
Palmitic acid	87.00	-5.42	236.13	132.20	0.51	-1.46	-2	1	-3.26
Gallic acid	41.20	-0.75	9.53	4.12	-0.98	-1.70	-2	3	-1.51
Bufotenine	82.15	-1.60	341.03	171.09	-0.10	-0.06	1	3	-5.07
Serotonin	64.59	-0.14	108.31	49.52	-0.54	-0.43	-1	4	-4.56
Tryptamine	80.60	-0.50	394.49	200.26	-0.36	0.09	1	3	-4.79
N, N-dimethyl-5-methoxy tryptamine	96.34	-1.99	1166.19	646.24	0.08	0.42	1	3	-4.85
Beta-sitosterol	100.00	-8.19	3438.01	1879.47	1.96	-0.33	0	3	-4.50
Myristic acid	95.25	-4.52	231.06	129.13	0.27	-1.28	-2	1	-2.89
Coumarin	94.30	-1.85	2036.82	1067.31	-0.55	0.01	1	0	-3.83
Nicotine	89.36	0.77	1262.08	703.87	-0.4	0.71	2	5	-4.43
Stigmasterol	100.00	-8.12	3418.01	1867.65	1.96	-0.26	0	5	-4.38
Vernolic acid	100.00	-5.07	238.78	133.80	0.31	-1.43	-2	3	-3.21
9H-Pyrido[3,4-B]indole	100.00	-2.74	3065.24	1660.20	-0.06	0.13	1	2	-4.47
6-methoxy-1-methyl-9H-pyrido[3,4-b]indole	100.00	-3.54	5308.77	2398.89	0.21	0.17	1	3	-4.50
Alpha-amyrenyl acetate	100.00	-8.12	4002.66	2215.22	2.35	0.13	1	2	-3.84
Ursolic acid	95.71	-6.94	363.23	210.57	1.34	-0.31	-1	3	-1.73
Betulinic acid	95.90	-6.82	346.51	200.11	1.34	-0.40	-1	3	-1.81

%HOA-%Huaman Oral Absorption, #metab-Number of likely metabolic reactions, QPlogS-Aqueous solubility, QPlogHERG-IC50 value for blockage of HERG K+channels, QPlog Caco-Apparent Caco-2 cell permeability, QPlogBB-Brain/Blood partition coefficient, CNS-Central Nervous System activity, QPlogKhsa-Binding to human serum albumin, QPlog MDCK-apparent Madin-Darby canine kidney (MDCK) cell permeability

For the development of oral drug candidates, % Human Oral Absorption (% HOA) is an important parameter. The recommended range for well-absorbed oral candidates is more than 80% and less than 20%, indicating poorly absorbed candidates. Most compounds showed moderate to good %HOA; glutathione is a poorly absorbed candidate, offering 0% %HOA. The compounds arachidic acid, sterol, beta-sitosterol, vernolic acid, 9H-Pyrido[3,4-B]indole, 6-methoxy-1-methyl-9H-pyrido[3,4-b]indole, alpha-amyrenyl acetate and stigmasterol show 100% %HOA.

QPlogS forecasts aqueous solubility, represented by log S, where S in mol dm^−3 denotes the solute concentration in equilibrium with the crystalline solid. The acceptable QPlogS range spans from -6.5 to -0.5. However, phytoconstituents such as beta-sitosterol,

stigmasterol, nicotine, alpha-amyrenyl acetate, ursolic acid, and betulinic acid exhibit QPlogS values slightly more than the designated range.

Caco-2 cells, derived from human colorectal carcinoma, represent differentiated intestinal cell lines exhibiting morphological and functional characteristics akin to *in vivo* intestinal epithelial cell barrier. The model helps to suggest the non-active transport of the molecule. The cell permeability value exceeding 500 suggests high, while the value below 25 indicates low permeability. The compounds levodopa, gallic acid, and glutathione showed poor Caco-2 cell permeability.

MDCK permeability descriptor gives the rapid permeability of the compound; they mimic BBB for nonactive transport. The recommended range for permeability is>500 nm/sec implies great, and<25 nm/sec indicates poor permeability. The sterol, N, N-dimethyltryptamine, beta-sitosterol, N, N-dimethyl-5-methoxytryptamine, stigmasterol, nicotine, and coumarin show higher MDCK permeability.

Prediction of plasma-protein binding: The effectiveness or biological impact of the medication is contingent on the extent of Plasma Protein Binding (PPB). QPlogKhsa assesses the binding of the ligands to serum albumin (preferable range-1.5 to 1.5). Beta-sitosterol, stigmasterol, and glutathione exhibit elevated QPlogkhsa values.

Prediction of Blood-Brain Barrier (BBB) penetration: The ability to penetrate the BBB is a crucial parameter in the pharmaceutical industry, especially for compounds that affect CNS. Conversely, inactive compounds in the CNS should not cross the barrier to prevent unintended effects in the CNS. In the test ligands, all compounds showed the predicted BBB permeability values ranging from –3.0 to 1.2. The permissible range for CNS activity is from-2 to+2. All the phytoconstituents exhibited CNS activity since their predicted CNS values fell within this allowable range.

Metabolism prediction (#metab) represents the number of metabolic reactions the compound may likely undergo. The recommended range for #metab is 1-8. Phytoconstituents like levodopa and glutathione will likely experience more than five reactions.

Predicted QPlogHERG gives IC_{50} value for blockage of HERG (Human Ether-a-go-go Related Gene) K+channels, which predicts early-stage cardiac toxicity of the drug. The phytoconstituents show the expected IC_{50} value within the standard range of five. Hence, it is anticipated not to cause any cardiac toxicity.

Toxicity prediction

The *in silico* toxicity prediction helps predict chemical compounds' potential toxicity. The predicted data is given in table 5.

Table 5: The predicted toxicity of the phytoconstituents

Phytoconstituents	Carcinogenicity	Mutagenicity	Hepatotoxicity	Neurotoxicity	Cytotoxicity	Clinical toxicity	Predicted LD50 (Mg/Kg)	Toxicity class
Luteolin	Inactive	Active	Inactive	Inactive	Inactive	Inactive	3919	4
Acacetin	Inactive	Inactive	Inactive	Inactive	Inactive	Active	4000	5
Arachidic acid	Inactive	Inactive	Inactive	Inactive	Inactive	Inactive	900	4
Genistein	Inactive	Inactive	Inactive	Inactive	Inactive	Inactive	2500	5
Sterol	Inactive	Inactive	Inactive	Inactive	Inactive	Inactive	500	4
Oleic acid	Inactive	Inactive	Inactive	Inactive	Inactive	Inactive	48	2
N,N-dimethyltryptamine	Inactive	Inactive	Inactive	Active	Inactive	Inactive	225	3
Dopamine	Inactive	Active	Inactive	-	-	-	2859	5
Stearic acid	Inactive	Inactive	Inactive	Inactive	Inactive	Inactive	900	4
Linoleic acid	Inactive	Inactive	Inactive	Inactive	Inactive	Inactive	10000	6
Glutathione	Inactive	Active	Inactive	Inactive	Inactive	Inactive	5000	5
Levodopa	Inactive	Inactive	Inactive	Inactive	Inactive	Active	1460	4
Ascorbic acid	Inactive	Inactive	Inactive	Inactive	Inactive	Active	3367	5
Palmitic acid	Active	Inactive	Inactive	Inactive	Inactive	Inactive	5000	5
Gallic acid	Active	Inactive	Inactive	Inactive	Inactive	Active	2000	4
Bufotenine	Inactive	Inactive	Inactive	Active	Inactive	Active	787	4
Serotonin	Inactive	Inactive	Inactive	Active	Inactive	Inactive	2300	5
Tryptamine	Inactive	Inactive	Inactive	Active	Inactive	Inactive	940	4
N, N-Dimethyl-5-methoxytryptamine	Inactive	Inactive	Inactive	Active	Inactive	Inactive	963	4
Beta-sitosterol	Inactive	Inactive	Inactive	Active	Inactive	Inactive	890	4
Myristic acid	Inactive	Inactive	Inactive	Inactive	Inactive	Inactive	900	4
Coumarin	Active	Inactive	Inactive	Active	Active	Inactive	196	3
Nicotine	Inactive	Inactive	Inactive	Active	Inactive	Active	3	1
Stigmasterol	Inactive	Inactive	Inactive	Active	Inactive	Inactive	890	4
Vernolic acid	Inactive	Inactive	Inactive	Inactive	Inactive	Inactive	5000	5
9H-Pyrido[3,4-B]indole	Inactive	Active	Inactive	Active	Inactive	Inactive	260	3
6-methoxy-1-methyl-9H-pyrido[3,4-b]indole	Inactive	Active	Inactive	Active	Inactive	Inactive	1230	4
Alpha-amyrenyl acetate	Active	Inactive	Inactive	Active	Inactive	Inactive	3460	5
Ursolic acid	Active	Inactive	Active	Inactive	Inactive	Active	2000	4
Betulinic acid	Active	Inactive	Inactive	Inactive	Inactive	Active	2610	5

Carcinogenicity and mutagenicity: The compounds other than palmitic acid, gallic acid, coumarin, alpha-prenyl acetate, ursolic acid, and betulinic acid demonstrated positive results for predicted carcinogenicity and the rest of the compounds non-carcinogenic nature [37]. Mutagenicity evaluates the potential of a substance to induce mutations in the biological system. Among the bioactive luteolin, dopamine, glutathione, 9H-pyrido[3,4-B]indole, 6-methoxy-1-methyl-9H-pyrido[3,4-b]indole exhibit positive results for ames mutagenesis.

Hepatoxicity is a significant factor in drug design because the liver plays a pivotal role in drug metabolism and detoxification [37]. Among the phytoconstituents, only ursolic acid displays hepatotoxicity. Hence, these constituents are predicted not to cause any risks associated with liver injury.

Neurotoxicity and cytotoxicity: Among the phytoconstituents, bufotenine, serotonin, tryptamine, N, N-dimethyl-5-methoxytryptamine, beta-sitosterol, coumarin, nicotine, stigmasterol, 9H-Pyrido[3,4-B]indole, 6-methoxy-1-methyl-9H-pyrido[3,4-b]indole, alpha-amyrenyl acetate showed the neurotoxicity. Most of the bioactive present in the *Mucuna pruriens* are non-cytotoxic. Among these, only coumarin was found to show cytotoxicity. Hence, these compounds do not show any toxicity to the cell.

Clinical Toxicity: Predicting clinical toxicity is essential to understand the compound's adverse side effects. Compounds like acacetin, levodopa, ascorbic acid, nicotine, ursolic acid, and betulinic acid are predicted to show clinical toxicity.

Predicted LD_{50} and acute oral toxicity

Most of the compounds exhibited LD_{50} ranges above 500 mg/kg, hence the compounds can be considered low toxic [37]. The constituents like oleic acid, N, N-dimethyltryptamine, coumarin, and nicotine exhibited LD_{50} ranges below 500 mg/kg, hence considered toxic. The higher the toxicity class, the lower the toxicity of the compounds. Most compounds fall under category three and above for acute oral toxicity, suggesting their relative safety for oral administration. The phytoconstituents like oleic acid and nicotine belong to classes 2 and 1, respectively, and are considered to be toxic.

Molecular docking studies

Molecular docking investigations were conducted to assess how the phytoconstituents interact with the active site of the enzyme MAO-B(2V5Z), AChE (4BDT), and COMT (3A7E).

The docking score indicates that the phytoconstituent has a significant affinity for the targets, as illustrated in table 6, and the interaction of the constituents with targets is given in table 7. Among the phytoconstituents of *Mucuna pruriens,* luteolin and acacetin showed an excellent binding affinity with multitargets.

Table 6: Docking score and ΔG bind of the phytoconstituents with target 2V5Z, 4BDT, and 3A7E

Phytoconstituent	MAO-B (2V5Z)		AChE (4BDT)		COMT (3A7E)	
	Docking score (Kcal/mol)	ΔG bind (Kcal/mol)	Docking score (Kcal/mol)	ΔG bind (Kcal/mol)	Docking score (Kcal/mol)	ΔG bind (Kcal/mol)
Luteolin	-11.504	-51.88	-11.443	-52.23	-6.518	-39.69
Acacetin	-10.620	-66.90	-9.850	-48.57	-4.824	-46.87
Arachidic acid	-10.500	-98.60	-8.617	-34.40	-	-
Genistein	-10.279	-54.29	-9.300	-54.26	-4.407	-32.90
Sterol	-9.860	-58.56	-8.409	-39.71	-3.122	-44.83
Oleic acid	-9.756	-96.22	-5.092	-50.07	-2.401	-54.77
N, N-Dimethyltryptamine	-8.735	-35.64	-8.672	-21.01	-3.218	-23.90
Dopamine	-8.731	-31.42	-7.565	-25.19	-3.845	-24.84
Stearic acid	-8.678	-91.85	-5.194	-26.03	-2.267	-54.19
Linoleic acid	-8.584	-95.48	-6.297	-49.65	-2.089	-59.75
Glutathione	-8.529	-63.06	-9.304	-43.19	-4.211	-35.38
Levodopa	-8.501	-33.50	-8.827	-27.75	-5.740	-28.14
Ascorbic acid	-8.469	-41.44	-6.828	-32.70	-4.873	-28.98
Palmitic acid	-8.141	-84.46	-5.876	-48.57	-2.057	-54.43
Gallic acid	-8.098	-33.23	-8.840	-32.66	-4.717	-25.77
Bufotenine	-7.921	-38.45	-6.901	-28.40	-3.291	-38.10
Serotonin	-7.646	-26.42	-7.617	-26.39	-3.863	-19.31
Tryptamine	-7.481	-32.50	-8.811	-14.06	-3.583	-25.05
N, N-Dimethyl-5-methoxytryptamine	-7.440	-38.57	-7.193	-23.17	-2.440	-41.50
Beta-sitosterol	-7.087	-88.03	-	-	-2.076	-51.97
Myristic acid	-7.080	-71.98	-5.221	-39.05	-2.418	-52.55
Coumarin	-7.008	-38.10	-7.476	-39.30	-2.911	-26.95
Nicotine	-6.296	-43.78	-4.833	-15.27	-3.238	-53.20
Stigmasterol	-6.168	-94.60	-	-	-2.567	-45.21
Vernolic acid	-6.104	-90.90	-7.720	-34.47	-2.977	-62.11
9H-Pyrido[3,4-B]indole	-7.805	-41.38	-8.683	-35.39	-3.493	-32.51
6-methoxy-1-methyl-9H-pyrido[3,4-b]indole	-7.682	-50.69	-9.074	-35.39	-5.313	-31.46
Alpha-amyrenyl acetate	-	-	-	-	0.540	-40.68
Ursolic acid	-	-	-	-	-0.684	-51.96
Betulinic acid	-	-	-	-	-2.523	-53.91

Among phytoconstituents, luteolin and acacetin achieved excellent docking scores of-11.504 and-10.620 kcal/mol, respectively, with MAO-B, whereas the levodopa exhibited a docking score of-8.501 kcal/mol. Luteolin made a strong hydrogen bonding with amino acid residues Tyr 188 and Gly 434. It also exhibited non-covalent interaction like hydrophobic interaction with amino acid residues Ile 198, Ile 199, Phe 168, Leu 171, Cys 172, Tyr 188, Tyr 398, Tyr 60, Tyr 326, Tyr 435 Met 436, Phe 343 and π-π interaction with amino acid residue Tyr 435. The acacetin formed four hydrogen bonds with Tyr 60, Ser 59, Gly 434, and Tyr 188, and hydrophobic interaction with amino acid residues Tyr 326, Ile 199, Phe 168, Ile 198, Leu 171, Tyr 435, Cys 172, Tyr 188, Tyr 398, Tyr 60, Met 436, Phe 343 along with the π-π interaction with amino acid residue Tyr435. The 2D and 3D images of the molecular interaction of phytochemicals, luteolin, and acacetin with the target 2V5Z are given in fig. 1 and 2.

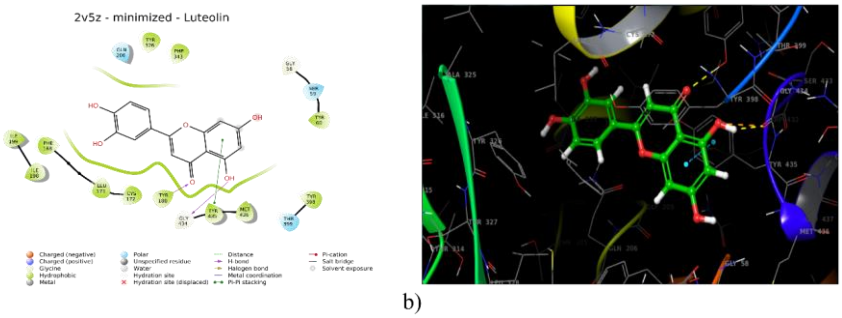

a) b)

Fig. 1: Represents 2D and 3D interaction of luteolin with 2V5Z

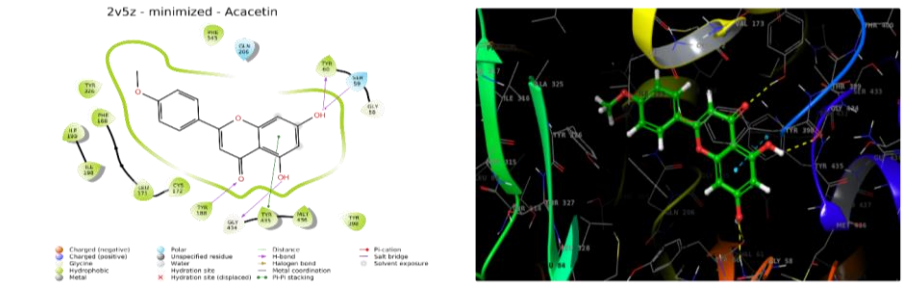

Fig. 2: Represents 2D and 3D interaction of acacetin with 2V5Z

Luteolin and acacetin exhibited the most favourable docking scores of-11.443 and-9.850 kcal/mol, respectively, when interacting with the target AChE (4BDT); the interaction diagram of luteolin and acacetin is given in fig. 3 and 4. Both acacetin and luteolin demonstrated polar interactions with His 447, Thr 83, and Ser 125 residues within the enzyme's active site. Additionally, their aromatic rings engaged in π-π stacking interactions with amino acid residues Trp 86 and Tyr 337 and also formed two hydrogen bonds with Gly 120 and Ser 125 residues. The hydrophobic interactions involved Tyr 133, Tyr 124, Trp 86, Tyr 341, Met 443, Trp 439, Pro 446, Tyr 449, and Tyr 337 residues. Notably, luteolin formed an additional hydrogen bond with His 447 and engaged in a hydrophobic interaction with Tyr 119, enhancing its binding affinity to the target, thereby implicating their potential efficacy.

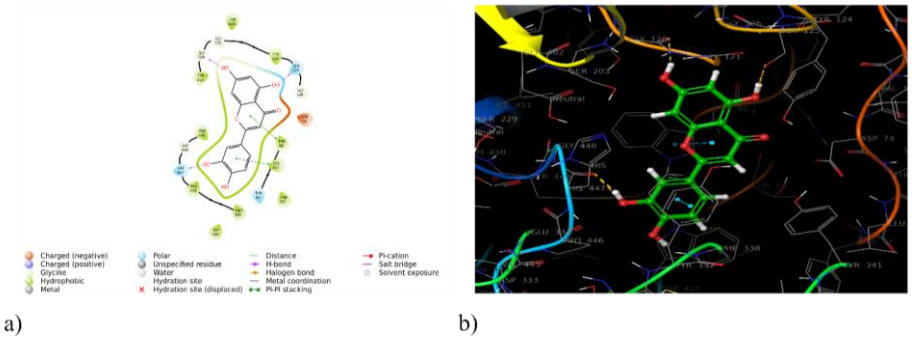

Fig. 3: Represents 2D and 3D interaction of luteolin with 4BDT

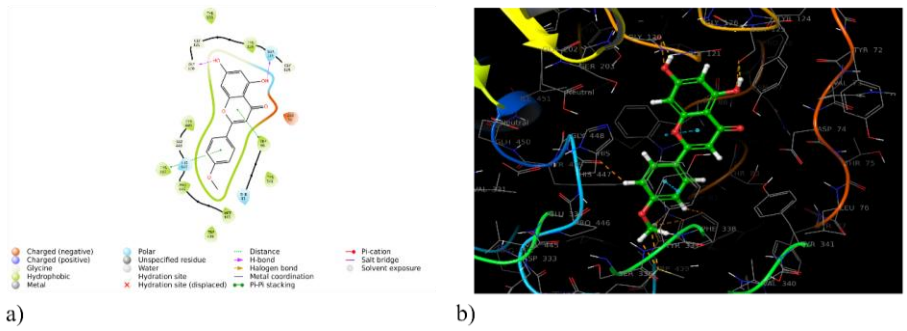

Fig. 4: Represents 2D and 3D interaction of acacetin with 4BDT

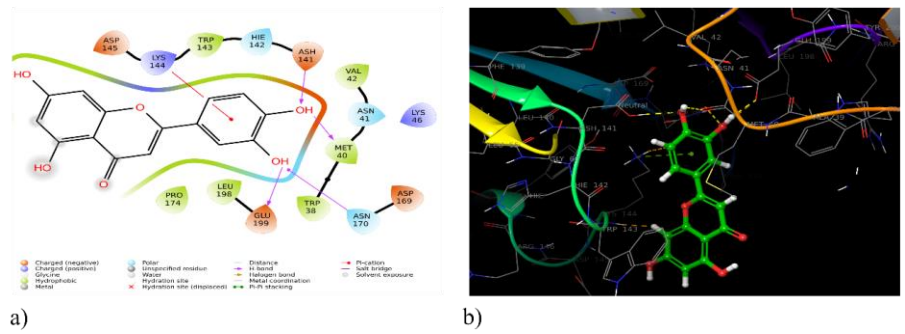

Fig. 5: Represents 2D and 3D interaction of luteolin with 3A7E

In the docking study targeting COMT (3A7E), luteolin and levodopa exhibited notable binding affinities with docking scores of-6.518 and-5.740 kcal/mol, respectively (fig. 5 and 6). Acacetin displayed a docking score of-4.824 kcal/mol, as depicted in fig. 7. In the case of luteolin, the catechol's hydroxyl group formed four hydrogen bonds with Asn170, Met40, Glu199, and Ash141. Hydrophobic interactions contributing to COMT inhibition also involved Pro174, Trp38, Leu198, Met40, Val42, and Trp143 residues. Luteolin demonstrated polar interactions with residues Hie142, Asn41, and Asn170. In the binding mode of levodopa, the amino group engaged in a hydrogen bond with Glu90, while Met40 interacted with the hydroxyl group of the catechol ring. Hydrophobic interactions implicated residues Tyr68, Ala67, Trp143, Met40, Ile91, and Cys95. Levodopa also formed polar interactions with Hie142, Asn41, and Asn92 residues.

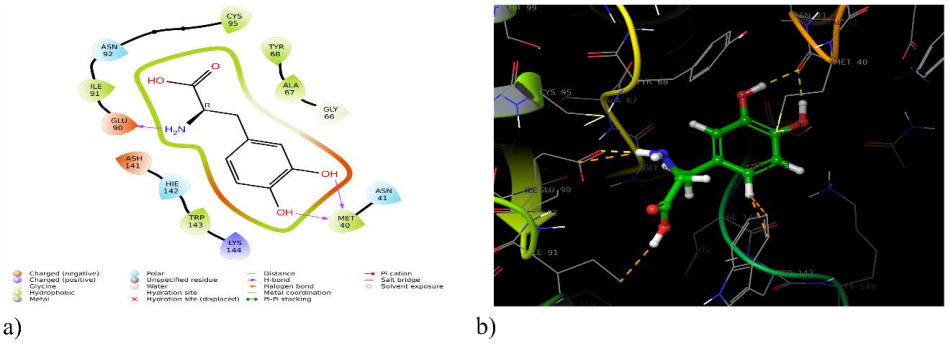

a) b)

Fig. 6: Represents 2D and 3D interaction of levodopa with 3A7E

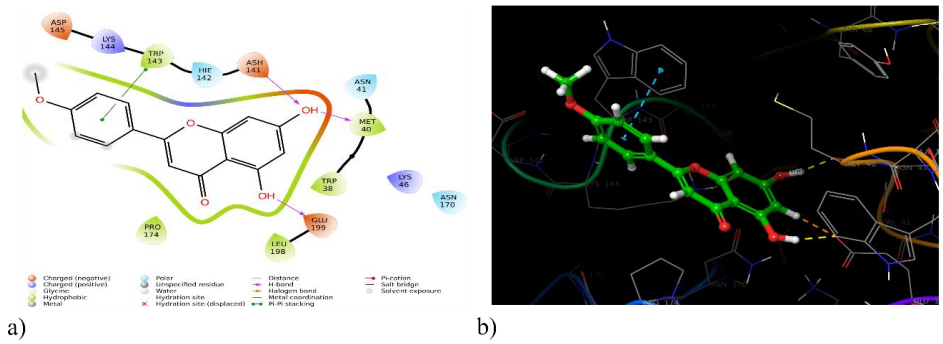

a) b)

Fig. 7: Represents 2D and 3D interaction of acacetin with 3A7E

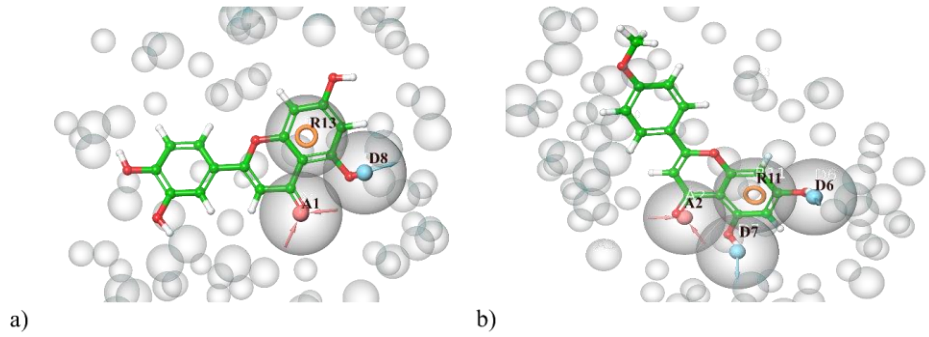

a) b)

Fig. 8: Pharmacophore models of a) Luteolin and b) Acacetin

Binding free energy calculation

The MMGBSA method helps validate the ligand-protein complexes' binding free energy. The binding energy of the phytoconstituents to the targets is given in table 6, and detailed energy terms favorable for interaction are listed in table 8. Among all of the interactions ΔG Coulomb, ΔG Hbond, ΔG Lipophilic, and ΔGVan der Waals energy, interactions accounted for inhibitory binding. The higher values of hydrophobic interactions in the negative range show its remarkable contribution to inhibitory action. The electrostatic solvation ΔG solvent GB and ΔG covalent energy terms are in the positive range; hence, these energy terms disfavour the binding of the compounds with the receptors.

The binding free energy ΔG binds for the MAO-B (2V5Z) enzyme ranges from-26.42 to -98.60 kcal/mol. The main contribution for enzyme electrostatic interaction ΔG bind Hbond, ΔG bind coulomb, ΔG bind Vander-waals and ΔG bind lipophilic, ranges from-0.01 Kcal/mol to-1.56 kcal/mol,-1.37 kcal/mol to-36.19 kcal/mol,-15.20 kcal/mol to-51.76 kcal/mol, and-102.95 kcal/mol to-14.77 kcal/mol respectively. The ΔG bind covalent and ΔG bind solvent are energy terms that disfavour the interactions.

The binding free energy ΔG binds for the AChE (4BDT) enzyme ranges from -14.06 to-52.23 kcal/mol. The phytoconstituent luteolin got the highest ΔG of -52.23 kcal/mol, indicating strong binding affinity.

The binding free energy ΔG binds for the COMT (3A7E) enzyme ranges from -19.31 to-59.75 kcal/mol. The compounds luteolin and acacetin have obtained ΔG binds values of -39.69 and-46.87 kcal/mol.

Table 7: Interactions of the phytoconstituents with targets 2V5Z, 4BDT, 3A7E

Phytoconstituents	Docking score (kcal/mol)	H bond	Polar interactions	Hydrophobic interaction	Pi-Pi stacking
Luteolin	2V5Z	Gly 434, Tyr 188	Thr 399, Ser 59, Gln 206	Ile 198, Ile 199, Phe 168, Leu 171, Cys 172, Tyr 188, Tyr 60, Met 436, Tyr 435, Tyr 398, Tyr 326, Phe 343	Tyr 435
	4BDT	His 447, Gly 120, Ser 125	His 447, Thr 83, Ser 125	Tyr 119, Tyr 133, Tyr 124, Trp 86, Tyr 337, Tyr 341, Met 443, Trp 439, Pro 446, Tyr 449	Trp 86, Tyr 337
	3A7E	Asn 170, Met 40, Glu 199, Ash 141	Hie 142, Asn 41, Asn 170	Pro 174, Trp 38, Leu 198, Met 40, Val 42, Trp 143	-
Acacetin	2V5Z	Tyr 60, Ser 59, Gly 434, Tyr 188	Gln 206, Ser 59,	Tyr 326, Phe 168, Ile 199, Ile 198, Leu 171, Cys 172, Tyr 188, Tyr 435, Met 436, Tyr 398, Tyr 60, Phe 343	Tyr 435
	4BDT	Gly 120, Ser 125	His 447, Thr 83, Ser 125	Tyr 133, Tyr 124, Trp 86, Tyr 341, Met 443, Trp 439, Pro 446, Tyr 449, Tyr 337	Trp 86, Tyr 337
	3A7E	Met 40, Ash 141, Glu 199	Hie 142, Asn 41, Asn 170	Pro 174, Leu 198, Trp 38, Met 40, Trp 143	Trp 143
Arachidic acid	2V5Z	Tyr 60, Ser 59	Gln 206, Ser 59	Tyr 326, Phe 99, Ile 316, Pro 102, Phe 103, Pro 104, Leu 164, Trp 119, Leu 167, Phe 168, Ile 199, Ile 198, Leu 171, Cyc 172 Phe 343, Tyr 398, Tyr 60, Val 61, Met 436, Tyr 435	-
	4BDT	Arg 296, Phe 295	His 447, Ser 125, Ser 203	Ala 204, Tyr 133, Val 294, Phe 295, Phe 297, Leu 298, Trp 286, Tyr 124, Trp 86, Met 443, Leu 437, Trp 439, Pro 446, Tyr 337, Tyr 449, Phe 338, Tyr 341	-
	3A7E	-	-	-	-
Genistein	2V5Z	Gly 434, Tyr 188	Gln 206, Thr 399, Ser 59	Tyr 60, Tyr 435, Tyr 398, Phe 343, Ile 199, Ile 198, Phe 168, Tyr 326, Leu 171, Cys 172, Tyr 188	Tyr 326, Tyr 435, Tyr 398
	4BDT	His 447	His 447, Ser 125, Asn 87, Thr 83	Tyr 449, Pro 446, Met 443, Trp 439, Tyr 337, Trp 86, Tyr 341, Tyr 124	Trp 86, Tyr 337
	3A7E	Asn 170, Ash 141	Asn 170, Hie 142	Pro 174, Cys 173, Leu 198, Trp 143, Met 40, Trp 38	-
Sterol	2V5Z	Gly 434	Gln 206	Phe 343, Le 328, Tyr 326, Ile 199, Ile 198, Cys 172, Leu 171, Phe 168, Phe 168, Tyr 188, Tyr 435, Tyr 60, Tyr 398	-
	4BDT	-	His 447, Ser 125, Thr 83, Asn 87	Tyr 449, Pro 446, Trp 439, Met 443, Tyr 337, Tyr 341, Trp 86, Tyr 124	-
	3A7E	-3.122	Ash 141	Asn 170, Hie 142	Leu 198, Cys 173, Pro 174, Trp 38, Met 40, Trp 143
Oleic acid	2V5Z	Tyr 60, Ser 59, Met 436	Ser 59, Gln 206	Trp 119, Leu 164, Pro 102, Phe 103, Pro 104, Leu 167, Phe 168, Ile 316, Ile 199, Ile 198, Leu 171, Cys 172, Tyr 398, Tyr 60, Val 61, Met 436, Ty R435, Phe 343	-
	4BDT	Arg 296, Phe 295	Ser 293, His 447, Thr 83, Ser 125	Trp 286, Leu 298, Phe 297, Phe 295, Val 294, Met 443, Pro 446, Trp 439, Tyr 449, Trp 86, Tyr 337, Phe 338, Tyr 341, Tyr 124	-
	3A7E	Ash 141	Hie 142, Ser 72, Asn 41, Asn 170	Val 42, Met 40, Trp 38, Trp 143, Phe 139, Tyr 71, Cys 69, Tyr 68, Ala 67, Val 203, Pro 174, Cys 173, Leu 198	-
N,N-dimethyltryptamine	2V5Z	Pro 102	Gln 206	Phe 99, Ile 316, Pro 102, Phe 103, Pro 104, Trp 119, Leu 164, Leu 167, Phe 168, Leu 171, Cys 172, Tyr 435, Ile 198, Ile 199, Tyr 326	-
	4BDT	His 447	His 447, Ser 125, Thr 83, Ser 203	Trp 86, Tyr 449, Pro 446, Tyr 337, Phe 338, Trp 439, Tyr 341, Tyr 124, Phe 297	Tyr 337, Trp 86
	3A7E	-	Asn 141, Ser 72, Hie 142, Asn 92	Phe 139, Trp 143, Ile 91, Cys 95, Tyr 68, Ala 67, Met 40	Trp 143
Dopamine	2V5Z	Tyr188, Cys17, Gly434, Tyr60	Thr399, Ser59	Tyr188, Cys172, Tyr435, Met436, Tyr398, Phe343, Tyr60	Tyr435, Tyr398
	4BDT	His 447, Asp 74, Tyr 337	His 447, Thr 83	Pro 446, Tyr 449, Trp 439, Trp 86, Tyr 337, Tyr 124, Tyr 341	Trp 86, Tyr 337
	3A7E	Ash 141, Asn 170, Glu 199	Asn 170, Asn 41, Hie 142	Trp 38, Met 40, Tyr 68, Trp 143, Pro 174	-
Stearic acid	2V5Z	Met 436, Tyr 60	Ser 59, Gln 206	Tyr 188, Tyr 435, Met 436, Tyr 60, Cys 172, Leu 171, Phe 168, Leu 167, Leu 164, Pro 104, Phe 103, Pro 102, Ile 316, Phe 343, Tyr 398, Trp 119, Ile 199, Ile 198, Tyr 326, Leu 328	-
	4BDT	Ser 125	Ser 203, His 447, Ser 125,	Ala 204, Tyr 133, Trp 86, Tyr 124, Tyr 72, Trp 286, Tyr 341, Phe 338, Tyr 337, Phe 295, Phe 297, Ile 451	-
	3A7E	Ser 72	Ser 72, Hie 142, Asn 92, Asn 141	Phe 139, Trp 143, Ile 91, Cys 95, Trp 38, Met 40, Val 42, Ala 67, Tyr 68, Cys 69, Tyr 71	-

Phytoconstituents	Docking score (kcal/mol)	H bond	Polar interactions	Hydrophobic interaction	Pi-Pi stacking
Linoleic acid	2V5Z	Ser 59, Tyr 60	Ser 200, Ser 59, Gln 206	Leu 164, Trp 119, Pro 102, Phe 103, Pro 104, Ile 316, Leu 328, Phe 343, Tyr 326, Tyr 398, Tyr 435, Met 436, Tyr 60, Val 61, Cys 172, Leu 171, Ile 199, Phe 168, Ile 198, Leu 167	-
	4BDT	Trp 86, Asp 74	Ser 203, Ser 125, Asn 87, Gln 71, Thr 83, His 447	Phe 295, Phe 297, Tyr 124, Pro 88, Trp 86, Tyr 72, Val 73, Tyr 449, Pro 446, Tyr 337, Phe 338, Trp 439, Tyr 341	-
	3A7E	Glu 199, Asn 170	Asn 170, Hie 142, Asn 92	Trp 38, Met 40, Leu 198, Cys 173, Pro 174, Trp 143, Ile 91, Tyr 68, Cys 85	-
Glutathione	2V5Z	Gly 434, Tyr 60, Gln 206, Ile 198	Gln 206, Ser 59, Thr 43, Thr 426, Thr 399	Ile 199, Ile 198, Tyr 60, Cys 172, Leu 171, Phe 168, Tyr 188, Met 436, Tyr 435, Tyr 398	-
	4BDT	Tyr 337, Ser 203, Tyr 124, Ser 125, Asp 74,	Ser 203, His 447, Ser 125, Thr 83	Tyr 337, Phe 338, Trp 439, Tyr 341, Trp 86, Tyr 124, Ile 451, Tyr 133, Phe 297, Ala 204	-
	3A7E	Gly 175, Asn 170, Glu 199	Asn 170	Pro 177, Ala 176, Pro 174, Trp 143, Met 40, Trp 38, Leu 198	-
Levodopa	2V5Z	Ser 59, Tyr 60, Tyr 435, Gln 206	Ser 59, Gln 65, Gln 206	Tyr 60, Val 61, Tyr 188, Tyr 398, Leu 171, Cys 172, Ile 198, Tyr 435, Met 436, Phe 343	Tyr 60
	4BDT	His 447, Asp 74	His 447, Ser 125, Thr 83, Asn 87	Pro 446, Tyr 449, Trp 439, Tyr 337, Trp 86, Tyr 124, Tyr 341,	Trp 86, Tyr 337
	3A7E	Met 40, Glu 90	Hie 142, Asn 41, Asn 92	Tyr 68, Ala 67, Trp 143, Met 40, Ile 91, Cys 95	-
Ascorbic acid	2V5Z	Gln 206, Tyr 435, Ser 59, Tyr 60	Ser 59, Gln 206	Cys 172, Leu 171, Ile 198, Tyr 435, Met 436, Tyr 188, Tyr 398, Tyr 60, Phe 343	-
	4BDT	His 447, Tyr 341	His 447, Thr 83	Pro 446, Tyr 449, Tyr 337, Trp 439, Tyr 341, Trp 86	-
	3A7E	Met 40, Ash 141, Glu 199	Asn 170, Asn 141, Hie 142	Pro 174, Leu 198, Trp 38, Met 40, Val 42, Trp 143	-
Palmitic acid	2V5Z	Tyr 60, Ser 59, Lys 296	Gln 206, Ser 59	Leu 164, Phe 343, Lue 167, Phe 168, Tyr 326, Leu 171, Cys 172, Tyr 398, Tyr 60, Phe 343, Tyr 435, Ile 198, Ile 199, Ile 316, Pro 102, Phe 103, Trp 119, Pro 104	-
	4BDT	Asn 87	Ser 203, Ser 125, Asn 87, Thr 83, His 447	Tyr 119, Ile 451, Tyr 449, Tyr 337, Pro 446, Met 443, Trp 439, Leu 437, Trp 86, Pro 88, Tyr 124, Val 73, Tyr 133	-
	3A7E	Ser 72	Ser 72, Hie 142, Asn 170, Asn 141	Phe 139, Trp 143, Cys 173, Pro 174, Val 203, Leu 198, Trp 38, Met 40, Val 42, Tyr 71, Cys 69, Tyr 68, Ala 67	-
Gallic acid	2V5Z	Gly 434, Tyr 188, Gln 206	Thr 399, Ser 59, Gln 206	Tyr 398, Tyr 435, Cys172, Tyr 188, Ile 198, Phe 343, Tyr 60	Tyr 435
	4BDT	His 447, Thr 83	His 447, Thr 83	Pro 446, Met 443, Trp 439, Tyr 337, Trp 86, Tyr 341, Tyr 449	Trp 86, Tyr 337
	3A7E	Glu 199, Met 40	Asn 170, Asn 141, Hie 142	Pro 174, Leu 198, Trp 38, Met 40, Trp 143	-
Bufotenine	2V5Z	Pro 102	Gln 206	Ile 316, Phe99, Tyr 326, Pro 102, Phe 103, Pro 104 Trp 119, Leu 164, Leu 167, Phe 168, Leu 171, Cys 172, Ile 199, Ile 198, Tyr 326, Phe 99	-
	4BDT	His 447	His 447, Thr 83, Ser 203	Ile 451, Tyr 133, Trp 86, Tyr 341, Tyr 337, Trp 439, Pro 446, Tyr 449, Ile 451	Trp 86, Tyr 337
	3A7E	Glu 199, Ash 141	Asn 170, Asn 41, Hie 142	Pro 174, Leu 198, Trp 38, Met 40, Trp 143	
Serotonin	2V5Z	Ile 199, Pro 102, Leu 164	Ser 200, Gln 206	Pro 102, Phe 103, Pro 104, Trp 119, Leu 164, Leu 167, Phe 168, Ile 316, Leu 171, Ile 198, Ile 199, Tyr 326	-
	4BDT	His 447, Asp 74	His 447, Ser 125, Thr 83	Tyr 341, Tyr 124, Tyr 449, Pro 446, Trp 86, Tyr 337, Trp 439	Trp 86, Tyr 337
	3A7E	Asn 170, Glu 199, Met 40, Ash 141	Asn 170, Asn 41, Hie 142	Trp 38, Leu 198, Met 40, Pro 174, Trp 143, Tyr 68	-
Tryptamine	2V5Z	Ile 199	Thr 201, Ser 200, Gln 206, Thr 314	Ile 199, Leu 328, Tyr 326, Leu 171, Phe 168, Leu 167, Leu 164, Trp 119, Pro 104, Phe 103, Pro 102, Phe 99, Leu 88, Ile 316	-
	4BDT	Thr 83, Tyr 341, His 447	His 447, Thr 83	Trp 86, Pro 446, Tyr 449, Tyr 337, Trp 439, Tyr 341, Met 443	Trp 86, Tyr 449, Tyr 337
	3A7E	Asn 170, Asp 169, Glu 199	Asn 41, Asn 170	Val 42, Met 40, Trp 38, Leu 198, Pro 174, Trp 173	-
N, N-Dimethyl-5-methoxytryptamine	2V5Z	-	Gln 206	Tyr 326, Ile 316, Pro 102, Phe 103, Pro 104, Leu 164, Trp 119, Phe 168, Ile 199, Ile 198, Leu 171, Cys 172, Tyr 188, Tyr 398, Tyr 435	Tyr 326
	4BDT	His 447	His 447, Thr 83, Ser 125, Asn 87	Trp 86, Tyr 449, Pro 446, Tyr 337, Tyr 341, Trp 439, Tyr 124	Trp 86, Tyr 337
	3A7E	-	Asn 170, Hie 142, Asn 41	Pro 174, Leu 198, Trp 38, Met 40, Val 42, Trp 143	-
Beta-sitosterol	2V5Z	-	Ser 59, Thr 426, Thr 43, Ser 59, Gln 206	Tyr 326, Leu 328, Phe 343, Tyr 398, Cys 397, Tyr 60, Ile 14, Ala 439, Met 436, Tyr 435, Gly 434, Tyr 188, Cys 172, Ile 198, Ile 199	-
	4BDT	-	-	-	-

Phytoconstituents	Docking score (kcal/mol)	H bond	Polar interactions	Hydrophobic interaction	Pi-Pi stacking
	3A7E	-	Hie 142, Asn 140	Trp 143, Leu 198, Met 40, Trp 38, Cys 173, Pro 174	-
Myristic acid	2V5Z	Tyr 60, Ser 59	Ser 59, Gln 206,	Phe 343, Cys 172, Leu 171, Trp 119, Ile 316, Phe 168, Leu 167, Leu 164, Tyr 326, Ile 199, Ile 198, Tyr 398, Met 436, Tyr 435, Val 61, Tyr 60,	
	4BDT	Glh 202, Tyr 133	Ser 203, His 447, Thr 83, Ser 125	Tyr 133, Leu 130, Tyr 119, Pro 446, Tyr 449, Ile 451, Trp 439, Tyr 337, Tyr 341, Trp 86, Tyr 124	-
	3A7E	Val 42, Ala67, Ser 72	Asn 41, Ser 72, Hie 142, Asn 92	Tyr 71, Met 40, Cys 69, Val 42, Tyr 68, Ala 67, Leu 65, Cys 95, Ile 91, Trp 143, Phe 139	
Coumarin	2V5Z	Tyr 60, Ser 59	Ser 59	Phe 343, Tyr 60, Met 436, Tyr 435, Tyr 188, Tyr 398, Cys 172, Leu 171	Tyr 398
	4BDT	Arg 296, Phe 295	Ser 293	Tyr 124, Phe 338, Tyr 337, Phe 297, Phe 295, Val 294, Leu 289, Trp 286, Tyr 341, Tyr 72	Trp 286
	3A7E	Ash 141	Asn 170, Hie 142	Leu 198, Trp 143, Pro 174, Trp 38, Met 40	-
Nicotine	2V5Z	Tyr 60, Ser 59	Ser 59	Tyr 188, Cys 172, Tyr 435, Met 436, Tyr 398, Phe 343, Tyr 60	Tyr 398
	4BDT	-	Asn 87, His 447, Thr 83, Ser 125	Tyr 449, Pro 446, Trp 439, Tyr 341, Tyr 337, Trp 86, Tyr 124	Trp 86, Tyr 337
	3A7E	-	Hie 142, Asn 92, Ser 119	Ala 118, Ile 89, Ile 91, Cys 95, Met 40, Tyr 68, Ala 67, Tyr 143	Trp 143
Stigmasterol	2V5Z	-	Thr 399, Gln 65, Gln 206, Ser 59, Thr 43, Thr 426	Ala 439, Ile 14, Tyr 60, Phe 343, Met 341 leu 328, Tyr 326, Ile 199, Ile 198, Cys 172, Leu 171, Cys 397, Tyr 398, Met 436, Tyr 435	-
	4BDT	-	-	-	-
	3A7E	Lys 144	Asn 170	Trp 143, Leu 198, Met 40, Trp 38, Cys 173, Pro 174	
Vernolic acid	2V5Z	Tyr 60, Ser 59	Ser 59, Gln 65, Gln 206, Thr 314, Thr 202, Thr201, Ser200	Phe 99, Leu 88, Pro 102, Phe 103, Pro 104, Trp 119, Leu 167, Phe 168, Leu 171, Cys 172, Tyr 188, Met 436, Tyr 435, Va L61, Tyr 60, Tyr 398, Phe 343, Ile 198, Ile 199, Ile 316, Tyr 326	-
	4BDT	Asn 87, Asp 74	Ser 125, Asn 87, Thr 83, Ser 203, His 447	Tyr 124, Pro 88, Trp 86, Val 73, Tyr 72, Tyr 337, Phe 338, Tyr 341, Trp 286, Phe 297, Phe 295	-
	3A7E	Ser 72	Asn 170, Hie 142, Ser 72, Asn 41	Phe 139, Trp 143, Val 203, Cys 173, Pro 174, Leu 198, Trp 38, Met 40val 42, Tyr 71, Cys 69, Tyr 68, Ala67	-
9H-Pyrido[3,4-B]indole	2V5Z	His 447	His 447, Thr 83	Met 443, Trp 86, Pro 446, Tyr 449, Trp 439, Tyr 337	Trp 86, Tyr 449, Tyr 337
	4BDT	His 447	His 447, Thr 83	Met 443, Trp 86, Pro 446, Tyr 449, Trp 439, Tyr 337	Trp 86, Tyr 449, Tyr 337
	3A7E	Glu 199	Hie 142, Asn 170	Leu 198, Trp 38, Met 40, Pro 174, Trp 143	Trp 38
6-methoxy-1-methyl-9H-pyrido[3,4-b]indole	2V5Z	Tyr 435, ser 59	Gln206, ser 59,	Ile 199, ile 198, phe 168, leu 171, cys 172, phe 343, tyr 60, met 436, tyr 435	Tyr 60
	4BDT	His 447	His 447, Ser 125, Thr 83	Tyr 337, Pro 446, Tyr 449, Tyr 133, Trp 86, Tyr 341, Trp 439	Trp 86, Tyr 337
	3A7E	Met 40	Asn 170, Asn 141, Hie 142	Trp 38, Met 40, Trp 143, Tyr 68, Ala 67, Ile 91, Pro 174	-
Alpha-amyrenyl acetate	2V5Z	-	-	-	-
	4BDT	-	-	-	-
	3A7E	Asp 145	-	Leu 198, Pro 174, Trp 143, Trp 38	-
Ursolic acid	2V5Z	-	-	-	-
	4BDT	-	-	-	-
	3A7E	Asp 145	Asn 170	Met 40, Trp 38, Pro 174, Trp 143	-
Betulinic acid	2V5Z	-	-	-	-
	4BDT	-	-	-	-
	3A7E	-	-	Pro 174, Trp 143, Met 40, Trp 38, Leu 198	-

Pharmacophore modelling

A pharmacophoric study was conducted on the compounds with the highest docking scores to validate the binding interactions. Pharmacophore modelling helps to validate and confirm the chemical interactions obtained from molecular docking studies [39]. The pharmacophoric features exposed by luteolin and acacetin are given in fig. 8. The pharmacophore modelling of luteolin reveals that the acceptor group A1 and donor group D8 are vital to interacting with the target. At the same time, the aromatic ring R13 assists in pi-pi stacking interaction with the target protein. These features were highlighted in the pharmacophore of acacetin along with an additional donor group D6 found in the acacetin pharmacophoric feature.

Table 8: MMGBSA binding free energy of the phytoconstituents with targets 2V5Z, 4BDT, 3A7E

Phytoconstituents	PDB ID	ΔG bind coulomb	ΔG bind covalent	ΔG bind H bond	ΔG bind lipophilic	ΔG bind solv GB	ΔG bind vander
Luteolin	2V5Z	-25.50	7.77	-0.92	-25.66	42.48	-43.83
	4BDT	-29.43	2.99	-0.70	-26.27	46.58	-30.72
	3A7E	-14.07	8.30	-1.42	-18.44	25.41	-33.49
Acacetin	2V5Z	-32.48	7.54	-0.84	-29.49	35.93	-43.01
	4BDT	-18.10	7.14	-0.47	-33.09	38.92	-29.48
	3A7E	-20.51	10.25	-1.51	-20.12	20.69	-31.05
Arachidic acid	2V5Z	-21.50	5.14	-0.65	-80.66	38.62	-39.55
	4BDT	-13.25	15.24	-0.55	-62.70	52.35	-25.47
	3A7E	-	-	-	-	-	-
Genistein	2V5Z	-17.32	0.31	-0.65	-26.37	30.48	-35.04
	4BDT	-20.66	1.22	-0.48	-27.10	34.72	-33.36
	3A7E	-13.04	4.19	-0.97	-20.05	29.57	-31.56
Sterol	2V5Z	-8.26	4.76	-0.24	-56.92	34.36	-32.27
	4BDT	-5.03	6.13	-0.25	-59.81	37.80	-18.55
	3A7E	-3.37	5.88	-0.33	-42.87	15.33	-19.49
Oleic acid	2V5Z	-20.31	7.67	-0.60	-69.03	32.35	-46.30
	4BDT	-19.66	11.21	-0.67	-51.32	34.65	-24.29
	3A7E	-25.05	13.05	-0.48	-52.55	38.31	-28.05
N, N-dimethyltryptamine	2V5Z	-6.24	4.46	-0.25	-37.52	33.91	-29.44
	4BDT	-6.51	1.75	-0.23	-23.35	49.41	-29.67
	3A7E	0.10	2.80	0.00	-30.91	31.85	-25.67
Dopamine	2V5Z	-28.93	5.52	-1.29	-16.93	27.90	-16.35
	4BDT	-16.10	-0.45	-1.37	-17.75	36.15	-20.81
	3A7E	-19.30	3.35	-2.31	-15.70	27.57	-17.99
Stearic acid	2V5Z	-19.99	7.82	-0.63	-67.60	37.13	-48.59
	4BDT	-8.53	10.05	-0.28	-51.19	41.54	-17.62
	3A7E	-15.35	7.45	-0.33	-43.02	31.41	-34.36
Linoleic acid	2V5Z	-19.16	3.62	-0.70	-69.04	35.92	-46.12
	4BDT	-5.86	0.62	-0.45	-52.29	54.77	-46.45
	3A7E	-7.87	-3.50	-0.93	-33.59	17.69	-31.55
Glutathione	2V5Z	-30.34	4.92	-1.56	-18.12	27.33	-45.30
	4BDT	-30.66	0.18	-2.12	-16.60	42.10	-36.09
	3A7E	-25.89	2.12	-2.04	-11.72	22.83	-20.68
Levodopa	2V5Z	-24.08	3.49	-1.36	-14.77	29.71	-25.79
	4BDT	-19.25	1.28	-1.92	-16.09	39.57	-25.29
	3A7E	-17.42	5.36	-1.92	-20.54	31.15	-24.77
Ascorbic acid	2V5Z	-35.26	2.50	-1.25	-14.02	24.47	-17.88
	4BDT	-14.09	1.18	-0.72	-19.21	19.89	-19.75
	3A7E	-10.10	1.48	-1.73	-14.04	15.14	-19.72
Palmitic acid	2V5Z	-12.78	5.38	-1.22	-63.49	30.89	-43.24
	4BDT	-11.59	3.94	-0.47	-50.12	45.27	-35.60
	3A7E	-14.25	8.34	-0.35	-47.88	35.43	-35.72
Gallic acid	2V5Z	-36.19	6.09	-1.21	-10.15	25.01	-15.20
	4BDT	-22.84	0.94	-0.70	-12.90	28.15	-21.08
	3A7E	-11.73	1.07	-2.81	-8.61	18.17	-21.62
Bufotenine	2V5Z	-10.00	3.09	-0.25	-38.88	36.43	-28.72
	4BDT	-8.55	1.40	-0.27	-26.68	48.94	-33.76
	3A7E	-17.38	2.66	-1.24	-20.25	23.45	-24.91
Serotonin	2V5Z	-9.26	0.34	-0.39	-29.68	36.32	-23.40
	4BDT	-16.46	0.74	-1.53	-19.67	45.35	-24.51
	3A7E	-21.53	7.91	-2.13	-17.94	28.90	-13.92
Tryptamine	2V5Z	-6.86	3.77	-0.50	-30.06	27.07	-25.26
	4BDT	-6.29	3.03	-0.68	-23.70	44.95	-22.09
	3A7E	-14.02	2.07	-2.20	-16.67	21.93	-15.56
N, N-Dimethyl-5-methoxytryptamine	2V5Z	-5.13	7.38	-0.23	-41.03	35.07	-34.23
	4BDT	-7.52	3.74	-0.24	-25.86	54.12	-35.10
	3A7E	-7.19	0.68	-0.85	-21.06	14.82	-27.57
Beta-sitosterol	2V5Z	-1.37	17.76	-0.01	-101.83	41.68	-44.27
	4BDT	-	-	-	-	-	-
	3A7E	-0.44	2.36	-0.98	-37.72	9.28	-24.47
Myristic acid	2V5Z	-21.93	5.98	-0.63	-49.98	29.52	-34.95
	4BDT	-10.54	7.74	-0.41	-45.84	38.63	-28.63
	3A7E	-24.22	10.46	-0.90	-45.55	37.43	-29.77
Coumarin	2V5Z	-10.03	0.15	-0.46	-14.95	14.67	-23.15
	4BDT	-12.79	-0.04	-0.41	-13.81	16.76	-19.94
	3A7E	0.69	0.05	-0.49	-12.75	7.95	-21.35
Nicotine	2V5Z	-13.23	0.60	-0.50	-23.90	13.77	-19.71
	4BDT	1.96	2.39	-0.03	-22.74	31.74	-24.18
	3A7E	-5.13	1.02	-0.07	-33.02	11.31	-25.20
Stigmasterol	2V5Z	-2.75	12.19	-0.01	-102.95	38.58	-39.66

Phytoconstituents	PDB ID	ΔG bind coulomb	ΔG bind covalent	ΔG bind H bond	ΔG bind lipophilic	ΔG bind solv GB	ΔG bind vander
	4BDT	-	-	-	-	-	-
	3A7E	-3.52	2.80	-0.77	-39.95	18.75	-22.51
Vernolic acid	2V5Z	-20.58	6.28	-0.69	-68.78	44.64	-51.76
	4BDT	-14.77	8.09	-0.54	-51.19	49.36	-25.42
	3A7E	-17.21	4.82	-0.35	-52.13	36.97	-34.20
9H-Pyrido[3,4-B]indole	2V5Z	-3.97	0.57	-0.09	-27.08	20.29	-29.88
	4BDT	-1.82	0.44	-0.21	-21.69	30.02	-25.41
	3A7E	-4.51	0.89	-1.55	-15.27	12.78	-23.59
6-methoxy-1-methyl-9H-pyrido[3,4-b]indole	2V5Z	-12.12	0.67	-0.56	-24.70	21.06	-32.60
	4BDT	1.12	3.48	-0.24	-27.34	35.51	-35.97
	3A7E	-8.31	2.44	-0.36	-26.14	29.54	-28.45
Alpha-amyrenyl acetate	2V5Z	-	-	-	-	-	-
	4BDT	-	-	-	-	-	-
	3A7E	-3.68	0.23	-0.16	-27.37	11.00	-20.70
Ursolic acid	2V5Z	-	-	-	-	-	-
	4BDT	-	-	-	-	-	-
	3A7E	-12.35	0.18	-0.96	-32.26	16.55	-23.13
Betulinic acid	2V5Z	-	-	-	-	-	-
	4BDT	-	-	-	-	-	-
	3A7E	0.84	0.46	-0.03	-41.96	12.58	-25.81

ΔG bind C ul mb-C ul mbenergy, Δ G bind c valent-C valent energy, ΔG bind Vander-Vander Waals energy, ΔG bind HB nd-Hydr genb ending energy, ΔG bind Lip phillic-Hydr ph bicenergy, ΔG bind S lvGB-*Electr statics lvati nenergy (p larc ntributi n*).

MD simulation

Among three targets, the compound luteolin and acacetin showed strong binding affinity towards MAO-B. Hence, those complexes were taken for MD simulation studies of 150 ns. Trajectory data was collected to assess the competitive inhibition and stability of the ligand-receptor complex. In addition to the dynamic simulation, 2D graphs depicting RMSD, RMSF, and hydrogen bonds were produced to comprehend the system's fidelity to its native motion during simulation. The RMSD (Root mean Square Deviation) plots of the co-crystal with the luteolin and acacetin complexes are depicted in fig. 9 and 10, respectively. The stability of the luteolin-bound MAO-B protein complex was investigated using molecular dynamic simulation studies. While analysing the RMSD values, a simulation lasting 150 ns revealed stable conformation. The RMSD was examined using the Cα atoms of the MAO-B protein and then plotted against the simulation time, as shown in fig. 9. When bound to MAO-B, luteolin displayed RMSD (Cα atom of MAO-B) values ranging from 2.0 to 3.0 Å with an average value of 1.70 Å. After the initial fluctuation in the equilibria, the RMSD for luteolin remained within the range of 1.5-3.0 Å until the simulation's conclusion. In the MD simulation study, the stability of the protein-ligand complex relies heavily on the behaviour of individual amino acid residues. The RMSF (Root mean Square Fluctuation) is utilised to evaluate the flexibility of each amino acid residue and the extent of its movement or alteration during the simulation duration. Fig. 10 displays the RMSF value calculated from the MD simulation trajectory. The literature analysis shows that a compound is considered a hit if it is firmly situated within the target protein's binding pocket (61), with minimal fluctuations observed in the active site atoms and main chain. The mean RMSF value of 0.66 Å for the Cα-atoms of the MAO-B protein bound to luteolin suggests minimal fluctuations in the complex structure, as indicated by the RMSF results.

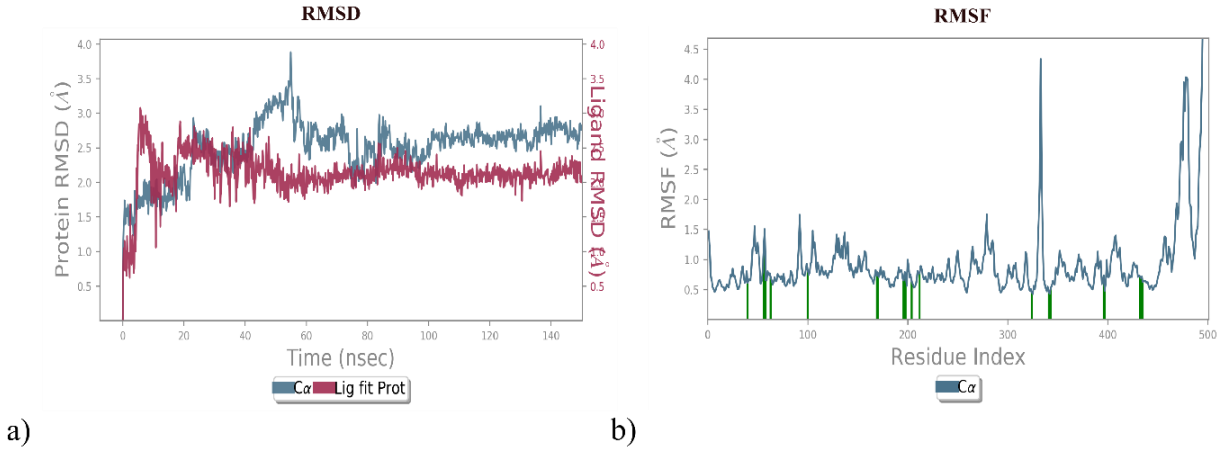

Fig. 9: MD simulation analysis of luteolin in complex with MAO B during 150 ns MD simulation time

Simulation studies were performed on the acacetin-bound MAO-B protein complex. The simulation initially showed instability up to 100 ns before confirming the RMSD values with stability. The RMSD was analysed utilising the Cα atoms of the MAO-B protein and plotted against the simulation time, as depicted in fig. 10. When bound to MAO-B, acacetin displayed RMSD (C atom of MAO-B) values ranging from 1.4 to 3.4 Å with an average value of 2.0 Å. During the 150-ns simulation, the compound acacetin's overall RMSD is within the acceptable range, supporting the stability of the protein-ligand complex. The mean RMSF value of the Cα atoms of the MAO-B of the MAO-B protein bound to acacetin was 0.55 Å, suggesting reduced fluctuation in the structure.

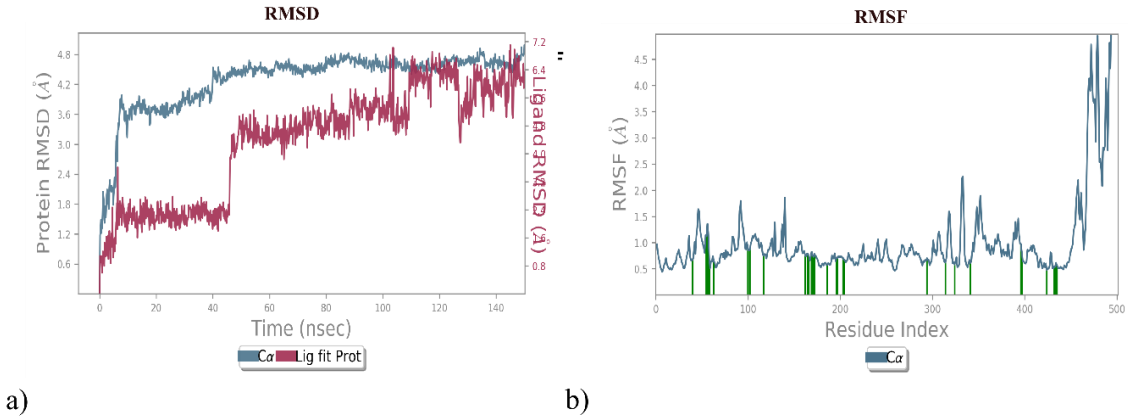

Fig. 10: MD simulation analysis of acacetin in complex with MAO B during 150 ns MD simulation time

Intermolecular contacts in molecular dynamic simulation

In the molecular dynamic simulation, a range of intermolecular interactions were observed, including hydrogen bonds, Van der Waals interactions, π-π stacking interactions, Dipole-dipole interactions, hydrophobic interactions, ionic interactions, Metal coordination, salt and water bridges. The fundamental interactions that the inhibitors demonstrate are illustrated in the stacked bar chart plots of luteolin and acacetin, as shown in fig. 7 and 8, respectively. The simulation interactions diagram also investigated more specific subtypes of each interaction type. The Tyr 60, Tyr 435 and Met 436 (hydrophobic) residue bounds to the aromatic ring and hydroxyl group, while Ser 200 have a polar charge and Gly 434 showed solvent exposure. The ligand luteolin-MAO-B simulation scored best, displaying H-bonds to the residues Tyr 60, Leu 171, Gln 206, Gly 434 and Met 436. Instead of these residues, other residues also took part in water bridges (Arg 47, Gly 58, Gln 65 and Ser 200). The Ile 199, Ty r326, Phe 343 and Tyr 435 contact with an inhibitor via hydrophobic interaction.

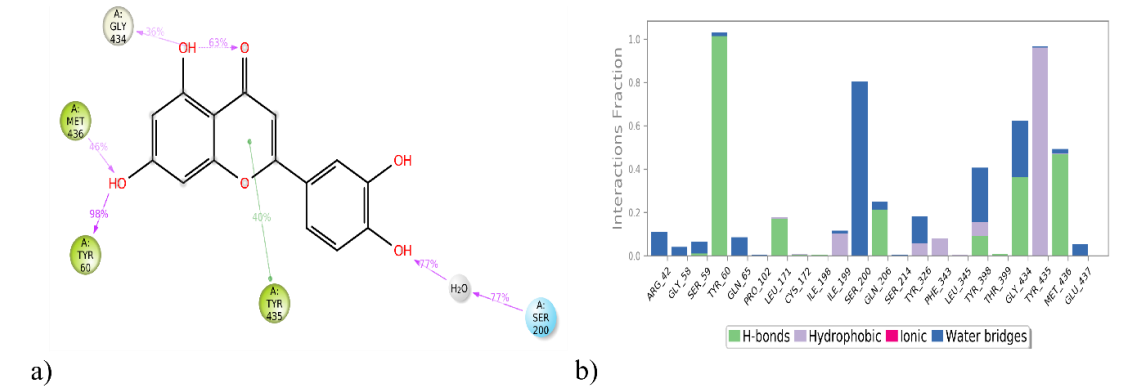

Fig. 11: Protein-ligand interaction of MAO B with luteolin

In 2D, MAO-B with acacetin in its active pocket developed hydrophobic contact with the amino acid residues Leu 171, Tyr 326 and Ile 199, resulting in a more robust interaction than luteolin. Ser 59, Cys 177, Gly 205, Lys 296, Thr 399 and Gly 434 explored water bridge interactions, and most residues appear in hydrogen bonds during simulation. Hydrogen bond interactions were calculated between residues (Tyr 60, Ile 198 and Met 436) and inhibitors. The hydrophobic interaction is Leu 171, Phe 168, Ile 316, Tyr 326, Ile 199 and Phe 343.

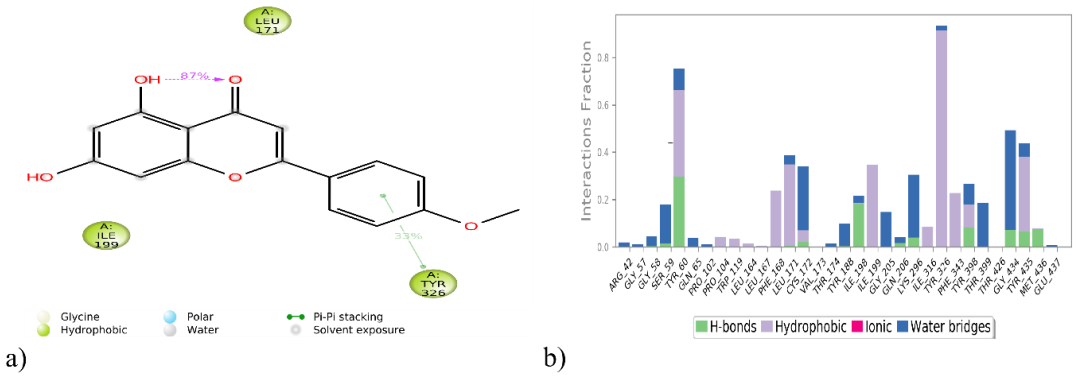

Fig. 12: Protein-ligand interaction of MAO B with acacetin

PASS prediction of the phytoconstituent

The result is generally represented as Pi and Pa, which gives the probability for the activity and inactivity of the compound, respectively. The compound is considered active and an analogue of the known drug if the Pa value exceeds 0.7. If the value ranges between 0.5<Pa<0.7, the compound may not show activity and have less or no structural similarity with the known drug. The compound is inactive or novel active moiety if the Pa value is less than 0.5[39]. The PASS prediction profile for the phytoconstituent is tabulated in table 9.

Table 9: PASS prediction of best-docked compounds

Phytoconstituents	DOPA decarboxylase inhibitor	MAO inhibitor	Antidyskinetic	MAO B inhibitor	Acute neurologic disorders treatment	Antiparkinsonian
Luteolin	0.635	0.568	0.496	0.422	0.499	-
Acacetin	0.508	0.620	0.400	0.502	0.429	-
Arachidic acid	0.350	-	0.646	-	-	0.432
Genistein	0.539	0.341	-	0.233	-	0.188
Sterol	0.106	-	-	-	-	0.011
Oleic acid	0.263	-	-	-	-	0.032
N, N-dimethyltryptamine	0.209	0.107	-	-	-	0.531
Dopamine	0.544	0.178	0.749	0.089	-	0.067
Stearic acid	0.350	-	0.646	-	-	0.432
Linoleic acid	0.235	-	0.423	-	-	0.323
Glutathione	-	-	-	-	0.710	-
Levodopa	0.824	0.095	0.685		0.735	0.304
Ascorbic acid	0.200		0.347	-	0.894	0.138
Palmitic acid	0.180	-	0.433	-	0.468	0.520
Gallic acid	0.611	-	0.609	-	0.510	0.373
Bufotenine	0.374	0.188	-	-	0.401	0.408
Serotonin	0.537	0.111	0.320	-	0.468	0.320
Tryptamine	0.369	0.099	0.323	-	0.450	0.412
N, N-Dimethyl-5-methoxy tryptamine	0.172	0.143	-	-	-	0.371
Beta-sitosterol	-	-	-	-	-	0.427
Myristic acid	0.350	-	0.646	-	0.562	0.432
Coumarin	0.274	0.475	0.602	0.379	0.373	0.432
Nicotine	-	-	0.301	-	0.297	0.513
Stigmasterol	-	-	-	-	-	0.622
Vernolic acid	-	-	0.293	-	0.354	0.155
9H-Pyrido[3,4-B]indole	0.159	-	0.300	-	0.438	0.210
6-methoxy-1-methyl-9H-pyrido[3,4-b]indole	-	0.087	0.268	-	1	0.207
Alpha-amyrenyl acetate	-	-	-	-	-	0.212
Ursolic acid	-	-	-	-	-	-
Betulinic acid	-	-	-	-	-	-

Table 10: Predicted targets for luteolin

Targets	Target class
NADPH oxidase 4	Enzyme
Aldose reductase	Enzyme
Cyclin-dependent kinase 5/CDK5 activator 1	Kinase
Xanthine dehydrogenase	Oxidoreductase
Monoamine oxidase A	Oxidoreductase
Tyrosine-protein kinase receptor FLT3	Kinase
Carbonic anhydrase II	Lyase
Cyclin-dependent kinase 1/cyclin B	Other cytosolic protein
Arachidonate 5-lipoxygenase	Oxidoreductase
Adenosine A1 receptor (by homology)	Family A G protein-coupled receptor
Carbonic anhydrase VII	Lyase
Glyoxalase I	Enzyme
Beta-amyloid A4 protein	Membrane receptor
Tyrosine-protein kinase SYK	Kinase
Glycogen synthase kinase-3 beta	Kinase
Poly [ADP-ribose] polymerase-1	Enzyme
Transthyretin	Secreted protein
Matrix metalloproteinase 9	Protease
Carbonic anhydrase XII	Lyase
Matrix metalloproteinase 2	Protease
Carbonic anhydrase IV	Lyase
Matrix metalloproteinase 12	Protease
Lymphocyte differentiation antigen CD38	Enzyme
Cytochrome P450 1B1	Cytochrome P450
ATP-binding cassette sub-family G member 2	Primary active transporter
Aldo-keto reductase family 1 member B10	Enzyme
Tankyrase-2	Enzyme
DNA topoisomerase I (by homology)	Isomerase
Arginase-1 (by homology)	Enzyme

Table 11: Predicted targets for acacetin

Target	Target class
Cytochrome P450 1B1	Cytochrome P450

Target prediction

Drug target prediction plays a crucial role in pharmaceutical discovery by elucidating the interactions between chemical compounds and protein targets within the human body. Computational methods for predicting these interactions are gaining popularity due to their cost-effectiveness and efficiency compared to traditional wet lab experiments. One such method is the Swiss Target Prediction website, which facilitates the estimation of the most probable macromolecular targets of a given small molecule with assumed bioactivity [40]. In this study, Swiss Target Prediction was employed to analyse the effects of luteolin and acacetin; the predicted targets showing the probability of 1 are tabulated in 10 and 11, respectively.

DISCUSSION

Researchers have noted that due to the intricate nature of PD, diagnostic success has been constrained. By investigating multiple signalling pathways, specific compounds derived from medicinal plants and dietary sources have exhibited promising efficacy in managing various NDs. Existing medications predominantly offer symptomatic relief and have demonstrated adverse effects in later life stages [41]. Consequently, plant-based medicine plays a crucial role by providing minimal side effects. Hence, the Ayurveda system of medicine is considered a practical and alternative approach to treatment. Various medicinal plants like *Mucuna pruriens, Withania somnifera,* and *Tinospora cordifolia* exhibit beneficial properties for treating neurodegenerative diseases [42-44].

This study selected thirty reported phytoconstituents of Mucuna pruriens for molecular docking studies. The phytoconstituents luteolin and acacetin have shown the highest binding affinity with the active site of multiple targets like MAO-B, AChE, and COMT. Overall, these findings underscore the significant molecular interactions of luteolin and acacetin with the multitarget, elucidating their potential as inhibitors through a combination of hydrogen bonding, hydrophobic interactions, and polar contacts. This information could be used to guide the design of more potent drug candidates for treating neurological disorders.

Chemically, luteolin is 3′, 4′, 5,7-tetrahydroxyflavone [45], and acacetin is 5,7-dihydroxy-4′-methoxyflavone [46]. In the case of luteolin, the 5,7-dihydroxy-4H-chromen-4-one is substituted with a catechol ring, whereas in acacetin, the anisole is attached, which is evident in pharmacophore modelling. The important pharmacophoric features of luteolin and acacetin responsible for the activity are the acceptor group, donor group, and aromatic ring. In the case of acacetin, an additional donor group (D6) is found, which may be responsible for the diminishment of activity compared to luteolin.

Bioactive such as luteolin gain significance due to their protective effects against oxidative stress and neuroinflammation, which contribute to the progression of PD [47]. Luteolin exerts its protective mechanisms against PD by modulating diverse signalling pathways, including the mitigation of oxidative stress [48] and neuroinflammation [49], inhibition of apoptosis, and facilitation of neuronal growth [50]. Additionally, various *in silico* studies confirm luteolin's capacity to impede the aggregation of alpha-synuclein, thus inhibiting the formation of Lewy bodies and potentially delaying the onset of advanced PD symptoms [51].

The Studies have investigated the potential capability of acacetin to inhibit the activation of the NLRP3 inflammasome, a crucial contributor to neuroinflammation, and have found that acacetin significantly suppresses inflammation in hyperactivated microglial cells [52]. Additionally, it has been observed to mitigate neuronal cell death and reduce microglial activation in a mouse model of ischemic stroke [53]. Consequently, these findings suggest that acacetin may act as a neuroprotective agent by inhibiting microglial activation, particularly in scenarios where microglial activation-induced inflammatory responses play a significant role in neuronal injury. Further validation of drug-protein interactions necessitates comprehensive pharmacological and clinical investigations.

CONCLUSION

Among the thirty phytoconstituents of *Mucuna pruriens*, most exhibited strong interactions with various targets relevant to PD, such as MAO-B, AChE, and COMT. The most active constituent, luteolin, demonstrated good binding affinity with a docking score of more than -6.0 kcal/mol, whereas acacetin exhibited a score above-4.0 kcal/mol with MAO-B, AChE, and COMT. Pharmacophore modelling predicts that essential pharmacophoric features such as donor, acceptor, and aromatic ring are critical for the activity. Compared to luteolin, the presence of an additional donor group in acacetin is responsible for the diminished activity. Among the three targets, the luteolin and acacetin showed high binding affinity against MAO-B. Consequently, a molecular dynamics study was carried out to better understand the binding mode and stability of these compounds towards the MAO-B. The study revealed that luteolin formed a more stable complex with MAO-B than acacetin. The physicochemical and ADME properties indicate that these compounds comply with the rule of five. Hence, these compounds can be considered as drug-like candidates. However, the major drawback of luteolin and acacetin is the presence of a hydrophilic hydroxyl group in their structure, resulting in lower CNS and BBB permeability. Thus, studies suggest that these compounds can be taken as a lead, and appropriate structural modification can be made to achieve more promising candidates, and *in vitro* and *in vivo* studies can be done for experimental validation of these compounds as potential drug for treating PD.

ACKNOWLEDGMENT

The authors acknowledge the CADD Lab of NGSM Institute of Pharmaceutical Sciences and express gratitude to Nitte Deemed to be University for providing facilities to carry out our study.

FUNDING

Nil

AUTHORS CONTRIBUTIONS

Zakiya Fathima C formulated the hypothesis, conducted the study, compiled the data, and wrote the original draft. Jainey P. James contributed to conceptualization, supervision, validation, and formal analysis of the manuscript. Mahendra Gowdru Srinivasa was contributed to perform the methodology. Mariyam Jouhara B. M reviewed and edited the manuscript. Sindhu T. J and B. C. Revanasiddappa performed formal analysis, while Sudeep D. Ghate contributed to the methodology.

CONFLICT OF INTERESTS

No potential conflict of interest

REFERENCES

1. Ouachinou JM, Dassou GH, Idohou R, Adomou AC, Yedomonhan H. National inventory and usage of plant-based medicine to treat gastrointestinal disorders with cattle in Benin (West Africa). S Afr J Bot. 2019;122:432-46. doi: 10.1016/j.sajb.2019.03.037.
2. Rai SN, Chaturvedi VK, Singh P, Singh BK, Singh MP. *Mucuna pruriens* in Parkinson's and in some other diseases: recent advancement and future prospective. 3 Biotech. 2020;10(12):522. doi: 10.1007/s13205-020-02532-7, PMID 33194526.
3. Lampariello LR, Cortelazzo A, Guerranti R, Sticozzi C, Valacchi G. The magic velvet bean of *Mucuna pruriens*. J Tradit Complement Med. 2012;2(4):331-9. doi: 10.1016/S2225-4110(16)30119-5, PMID 24716148.

4. Martinez Leo EE, Martin Ortega AM, Acevedo Fernandez JJ, Moo-Puc R, Segura Campos MR. Peptides from *Mucuna pruriens* L., with protection and antioxidant *in vitro* effect on HeLa cell line. J Sci Food Agric. 2019;99(8):4167-73. doi: 10.1002/jsfa.9649, PMID 30779130.
5. Guerranti R, Ogueli IG, Bertocci E, Muzzi C, Aguiyi JC, Cianti R. Proteomic analysis of the pathophysiological process involved in the antisnake venom effect of Mucuna pruriens extract. Proteomics. 2008;8(2):402-12. doi: 10.1002/pmic.200700265, PMID 18203263.
6. Sardjono RE, Khoerunnisa F, Musthopa I, Akasum NS, Rachmawati R. Synthesize, characterization, and anti-Parkinson activity of silver-Indonesian velvet beans (*Mucuna pruriens*) seed extract nanoparticles (AgMPn). J Phys.: Conf Ser. 2018;1013:012195, doi: 10.1088/1742-6596/1013/1/012195.
7. Majekodunmi SO, Oyagbemi AA, Umukoro S, Odeku OA. Evaluation of the anti–diabetic properties of *Mucuna pruriens* seed extract. Asian Pac J Trop Med. 2011;4(8):632-6. doi: 10.1016/S1995-7645(11)60161-2, PMID 21914541.
8. Golbabapour S, Hajrezaie M, Hassandarvish P, Abdul Majid N, Hadi AH, Nordin N. Acute toxicity and gastroprotective role of *M. pruriens* in ethanol-induced gastric mucosal injuries in rats. BioMed Res Int. 2013(1):974185. doi: 10.1155/2013/974185, PMID 23781513.
9. Avoseh ON, Ogunwande IA, Ojenike GO, Mtunzi FM. Volatile composition, toxicity, analgesic, and anti-inflammatory activities of *Mucuna pruriens*. Nat Prod Commun. 2020;15(7). doi: 10.1177/1934578X20932326.
10. Okpashi VE, Azuaga TI, Iyen SI, Aikhoje EF, Lajaka JI. Phytochemical screening and antimicrobial activities of leaf extracts of *Mucuna pruriens*. JOPHAS. OA U. 2019;16(4).
11. Menon S, Agarwal H, Rajeshkumar S, Kumar SV. Anticancer assessment of biosynthesized silver nanoparticles using *Mucuna pruriens* seed extract on lung cancer treatment. Res J Pharm Technol. 2018;11(9):3887-91. doi: 10.5958/0974-360X.2018.00712.6.
12. Suresh S, Prakash S. Effect of *Mucuna pruriens* (Linn.) on sexual behavior and sperm parameters in streptozotocin-induced diabetic male rat. J Sex Med. 2012;9(12):3066-78. doi: 10.1111/j.1743-6109.2010.01831.x, PMID 20456630.
13. Pulikkalpura H, Kurup R, Mathew PJ, Baby S. Levodopa in *Mucuna pruriens* and its degradation. Sci Rep. 2015;5(1):11078. doi: 10.1038/srep11078, PMID 26058043.
14. Wakabayashi K, Tanji K, Mori F, Takahashi H. The lewy body in Parkinson's disease: molecules implicated in the formation and degradation of α-synuclein aggregates. Neuropathology. 2007;27(5):494-506. doi: 10.1111/j.1440-1789.2007.00803.x, PMID 18018486.
15. Michalska P, León R. When it comes to an end: oxidative stress crosstalk with protein aggregation and neuroinflammation induce neurodegeneration. Antioxidants (Basel). 2020;9(8):740. doi: 10.3390/antiox9080740, PMID 32806679.
16. Mishra AK, Dixit A. Dopaminergic axons: key recitalists in Parkinson's disease. Neurochem Res. 2022;47(2):234-48. doi: 10.1007/s11064-021-03464-1, PMID 34637100.
17. Cheong SL, Federico S, Spalluto G, Klotz KN, Pastorin G. The current status of pharmacotherapy for the treatment of Parkinson's disease: transition from single-target to multitarget therapy. Drug Discov Today. 2019;24(9):1769-83. doi: 10.1016/j.drudis.2019.05.003, PMID 31102728.
18. Mathew B, Parambi DG, Mathew GE, Uddin MS, Inasu ST, Kim H. Emerging therapeutic potentials of dual-acting MAO and AChE inhibitors in Alzheimer's and Parkinson's diseases. Arch Pharmazie. 2019;352(11):e1900177. doi: 10.1002/ardp.201900177, PMID 31478569.
19. Morphy R, Rankovic Z. Designed multiple ligands. An emerging drug discovery paradigm. J Med Chem. 2005;48(21):6523-43. doi: 10.1021/jm058225d, PMID 16220969.
20. Alov P, Stoimenov H, Lessigiarska I, Pencheva T, Tzvetkov NT, Pajeva I. *In silico* identification of multi-target ligands as promising hit compounds for neurodegenerative diseases drug development. Int J Mol Sci. 2022;23(21):13650. doi: 10.3390/ijms232113650, PMID 36362434.
21. James JP, Aiswarya TC, Priya SN, Jyothi DI, Dixit SR. Structure based multitargeted molecular docking analysis of pyrazole-condensed heterocyclics against lung cancer. Int J App Pharm. 2021;3(6):157-69. doi: 10.22159/ijap.2021v13i6.42801.
22. Nugraha SE, Keliat JM, Marianne SRA. Investigating the toxicity of betalain compounds: *in silico* analysis and *in vivo* predictions for standardized *Beta vulgaris* L. extract. Int J App Pharm. 2024;16(1):118-23. doi: 10.22159/ijap.2024v16i1.49189.
23. James JP, Pramatha P, Jouhara M, Fathima C Z, D'Souza RR. Green synthesis, multitargeted molecular docking and ADMET studies of chalcones based scaffold as anti-breast cancer agents. Res J Pharm Technol. 2023;16(5):2215-22. doi: 10.52711/0974-360X.2023.00364.
24. Suwardi S, Salim A, Mahendra JA, Wijayanto DB, Rochiman NA, Anam SK. Virtual screening, pharmacokinetic prediction, molecular docking and dynamics approaches in the search for selective and potent natural molecular inhibitors of MAO-B for the treatment of neurodegenerative diseases. Indo J Chem Env. 2023;6(2):95-110. doi: 10.21831/ijoce.v6i2.68338.
25. Hosen ME, Rahman MS, Faruqe MO, Khalekuzzaman M, Islam MA, Acharjee UK. Molecular docking and dynamics simulation approach of *Camellia sinensis* leaf extract derived compounds as potential cholinesterase inhibitors. In Silico Pharmacol. 2023;11(1):14. doi: 10.1007/s40203-023-00151-7, PMID 37255739.
26. Patel CN, Georrge JJ, Modi KM, Narechania MB, Patel DP, Gonzalez FJ. Pharmacophore-based virtual screening of catechol-O-methyltransferase (COMT) inhibitors to combat Alzheimer's disease. J Biomol Struct Dyn. 2018;36(15):3938-57. doi: 10.1080/07391102.2017.1404931, PMID 29281938.
27. James JP, Jyothi D, Priya S. In silico screening of phytoconstituents with antiviral activities against SARS-COV-2 main protease, Nsp12 polymerase, and Nsp13 helicase proteins. Lett Drug Des Discov. 2021;18(8):841-57. doi: 10.2174/1570180818666210317162502.
28. Mateev E, Georgieva M, Zlatkov A. Improved molecular docking of MAO-B inhibitors with glide. Biointerface Res Appl Chem. 2022;13(2):159. doi: 10.33263/BRIAC132.159.
29. James P, Ishwar Bhat K, More UA, Joshi SD. Design, synthesis, molecular modeling, and ADMET studies of some pyrazoline derivatives as shikimate kinase inhibitors. Med Chem Res. 2018;27(2):546-59. doi: 10.1007/s00044-017-2081-9.
30. Malkaje S, Srinivasa MG, Deshpande NS, Navada S, Revanasiddappa BC. An in-silico approach: design, homology modeling, molecular docking, MM/GBSA simulations, and ADMET screening of novel 1,3,4-oxadiazoles as PLK1 inhibitors. Curr Drug Res Rev. 2023;15(1):88-100. doi: 10.2174/2589977514666220821203739, PMID 36017854.
31. Sachdeo R, Khanwelkar C, Shete A. *In silico* exploration of berberine as a potential wound healing agent via network pharmacology, molecular docking, and molecular dynamics simulation. Int J App Pharm. 2024;16(2):188-94. doi: 10.22159/ijap.2024v16i2.49922.
32. Lagunin A, Filimonov D, Poroikov V. Multi-targeted natural products evaluation based on biological activity prediction with pass. Curr Pharm Des. 2010;16(15):1703-17. doi: 10.2174/138161210791164063, PMID 20222853.
33. T SP, P James J, SR Dwivedi P, Priya S, Fathima CZ, T JS. Synthesis, molecular docking and molecular dynamic studies of thiazolidineones as acetylcholinesterase and butyrylcholinesterase inhibitors. Polycyclic Aromatic Compounds. 2024;44(5):3387-407. doi: 10.1080/10406638.2023.2233666.
34. James JP, Aziz AA, Krishnan D, Kumar P, Kumar A. Molecular docking and pharmacophore modelling of phytoconstituents of *Vaccinium secundiflorum* for antidiabetic and antioxidant activity. IJCBDD. 2021;14(5):315-42. doi: 10.1504/IJCBDD.2021.120122.
35. James JP, Devaraji V, Sasidharan P, Pavan TS. Pharmacophore modeling, 3D QSAR, molecular dynamics studies and virtual screening on pyrazolopyrimidines as anti-breast cancer agents. Polycyclic Aromatic Compounds. 2023 Sep 14;43(8):7456-73. doi: 10.1080/10406638.2022.2135545.
36. Muralikrishnan A, Kubavat J, Vasava M, Jupudi S, Biju N. Investigation of anti-SARS CoV-2 activity of some tetrahydro curcumin derivatives: an *in silico* study. Int J App Pharm. 2023;15(1):333-9. doi: 10.22159/ijap.2023v15i1.46288.

37. Banerjee P, Eckert AO, Schrey AK, Preissner R. ProTox-II: a web server for the prediction of toxicity of chemicals. Nucleic Acids Res. 2018;46(W1):W257-63. doi: 10.1093/nar/gky318, PMID 29718510.
38. Patel S, Modi P, Chhabria M. Rational approach to identify newer caspase-1 inhibitors using pharmacophore-based virtual screening, docking and molecular dynamic simulation studies. J Mol Graph Model. 2018;81:106-15. doi: 10.1016/j.jmgm.2018.02.017, PMID 29549805.
39. Filimonov DA, Lagunin AA, Gloriozova TA, Rudik AV, Druzhilovskii DS, Pogodin PV. Prediction of the biological activity spectra of organic compounds using the PASS online web resource. Chem Heterocycl Comp. 2014;50(3):444-57. doi: 10.1007/s10593-014-1496-1.
40. Daina A, Michielin O, Zoete V. Swiss target prediction: updated data and new features for efficient prediction of protein targets of small molecules. Nucleic Acids Res. 2019;47(W1):W357-64. doi: 10.1093/nar/gkz382, PMID 31106366.
41. Goldenberg MM. Medical management of Parkinson's disease. PT. 2008;33(10):590-606. PMID 19750042.
42. Rai SN, Birla H, Singh SS, Zahra W, Patil RR, Jadhav JP. *Mucuna pruriens* protects against MPTP-intoxicated neuroinflammation in Parkinson's disease through NF-κB/pAKT signaling pathways. Front Aging Neurosci. 2017;9:421. doi: 10.3389/fnagi.2017.00421, PMID 29311905.
43. Prakash J, Chouhan S, Yadav SK, Westfall S, Rai SN, Singh SP. *Withania somnifera* alleviates Parkinsonian phenotypes by inhibiting apoptotic pathways in dopaminergic neurons. Neurochem Res. 2014;39(12):2527-36. doi: 10.1007/s11064-014-1443-7, PMID 25403619.
44. Birla H, Rai SN, Singh SS, Zahra W, Rawat A, Tiwari N. *Tinospora cordifolia* suppresses neuroinflammation in Parkinsonian mouse model. Neuro Molecular Med. 2019;21(1):42-53. doi: 10.1007/s12017-018-08521-7, PMID 30644041.
45. Siddique YH. Role of luteolin in overcoming Parkinson's disease. BioFactors. 2021;47(2):198-206. doi: 10.1002/biof.1706, PMID 33443305.
46. Ha SK, Moon E, Lee P, Ryu JH, Oh MS, Kim SY. Acacetin attenuates neuroinflammation via regulation the response to LPS stimuli in vitro and in vivo. Neurochem Res. 2012;37(7):1560-7. doi: 10.1007/s11064-012-0751-z, PMID 22447574.
47. Siddique YH, Jyoti S, Naz F. Protective effect of luteolin on the transgenic Drosophila model of Parkinson's disease. Braz J Pharm Sci. 2018;54(3):1-13. doi: 10.1590/s2175-97902018000317760.
48. Huang L, Kim MY, Cho JY. Immunopharmacological activities of luteolin in chronic diseases. Int J Mol Sci. 2023;24(3):2136. doi: 10.3390/ijms24032136, PMID 36768462.
49. Elmazoglu Z, Yar Saglam AS, Sonmez C, Karasu C. Luteolin protects microglia against rotenone-induced toxicity in a hormetic manner through targeting oxidative stress response, genes associated with Parkinson's disease and inflammatory pathways. Drug Chem Toxicol. 2020;43(1):96-103. doi: 10.1080/01480545.2018.1504961, PMID 30207190.
50. Siracusa R, Paterniti I, Impellizzeri D, Cordaro M, Crupi R, Navarra M. The association of palmitoylethanolamide with luteolin decreases neuroinflammation and stimulates autophagy in Parkinson's disease model. CNS Neurol Disord Drug Targets. 2015;14(10):1350-65. doi: 10.2174/1871527314666150821102823, PMID 26295827.
51. Reudhabibadh R, Binlateh T, Chonpathompikunlert P, Nonpanya N, Prommeenate P, Chanvorachote P. Suppressing Cdk5 activity by luteolin inhibits MPP+-induced apoptotic of neuroblastoma through Erk/Drp1 and Fak/Akt/GSK3β pathways. Molecules. 2021;26(5):1307. doi: 10.3390/molecules26051307, PMID 33671094.
52. Ha SK, Moon E, Lee P, Ryu JH, Oh MS, Kim SY. Acacetin attenuates neuroinflammation via regulation the response to LPS stimuli *in vitro* and *in vivo*. Neurochem Res. 2012;37(7):1560-7. doi: 10.1007/s11064-012-0751-z, PMID 22447574.
53. Bu J, Shi S, Wang HQ, Niu XS, Zhao ZF, Wu WD. Acacetin protects against cerebral ischemia-reperfusion injury via the NLRP3 signaling pathway. Neural Regen Res. 2019;14(4):605-12. doi: 10.4103/1673-5374.247465, PMID 30632500.